

APPENDIX - FOR ONLINE PUBLICATION

Why Does the Fed Move Markets so Much? A Model of Monetary Policy and Time-Varying Risk Aversion

Carolin Pflueger and Gianluca Rinaldi¹

March 2021

¹Pflueger: University of Chicago, Harris School of Public Policy, NBER, and CEPR. Email cpflueger@uchicago.edu. Rinaldi: Harvard University. Email rinaldi@g.harvard.edu.

A Loglinear habit dynamics around steady state

This section derives the loglinear dynamics of the habit stock using a first order approximation around the steady state $S_t = \bar{S}$. We write log habit h_t as a distributed lag of moments of consumption, the habit shock $\varepsilon_{s,t}$, and the output gap, which also equals the deviation of log consumption from the frictionless level. This loglinear expansion therefore implies that we can broadly view habit as a function of (lags of) consumption moments, and the shock $\varepsilon_{s,t}$, which for this reason we refer to as a “habit shock”.

In the paper, we model how habit adjusts to consumption implicitly by modeling the evolution of the log surplus consumption ratio. In order to solve for log habit we need an approximate relation between log habit, log consumption, and the log surplus consumption ratio. Defining $\hat{s}_t = s_t - \bar{s}$, we develop a first-order Taylor expansion of \hat{s}_t in terms of $c_t - h_t$. We take the first derivative of \hat{s}_t with respect to $c_t - h_t$:

$$\frac{d\hat{s}_t}{d(c_t - h_t)} = \frac{d}{d(c_t - h_t)} \left(\log \left(\frac{1 - \exp(-(c_t - h_t))}{\bar{S}} \right) \right), \quad (\text{A1})$$

$$= \frac{\bar{S}}{1 - \exp(-(c_t - h_t))} \frac{\exp(-(c_t - h_t))}{\bar{S}}, \quad (\text{A2})$$

$$= - \left(1 - \frac{1}{\bar{S}} \right), \quad (\text{A3})$$

so at the steady state this first derivative equals:

$$\left. \frac{d\hat{s}_t}{d(c_t - h_t)} \right|_{s_t = \bar{s}} = - \left(1 - \frac{1}{\bar{S}} \right). \quad (\text{A4})$$

The first order Taylor expansion for \hat{s}_t in terms of $c_t - h_t$ around the steady-state therefore equals (up to constant):

$$\hat{s}_t \approx \left(1 - \frac{1}{\bar{S}} \right) (h_t - c_t), \quad (\text{A5})$$

or

$$h_t \approx c_t + \frac{\hat{s}_t}{1 - \frac{1}{\bar{S}}}. \quad (\text{A6})$$

The relation (A6) is approximate rather than exact because we ignore second- and higher-order terms in $(c_t - h_t)$. Further approximating $\lambda(s_t) \approx \lambda(\bar{s}) = \frac{1}{\bar{S}} - 1$, the approximate dynamics for \hat{s}_t near the steady state are given by:

$$\hat{s}_{t+1} \approx \theta_0 \hat{s}_t + \theta_1 x_t + \theta_2 x_{t-1} + \varepsilon_{s,t} + \left(\frac{1}{\bar{S}} - 1 \right) \varepsilon_{c,t+1}. \quad (\text{A7})$$

Combining (A6) with (A7) gives the approximate dynamics for log habit:

$$h_{t+1} \approx c_{t+1} + \frac{1}{1 - \frac{1}{S}} \hat{s}_{t+1}, \quad (\text{A8})$$

$$\approx c_{t+1} + \frac{1}{1 - \frac{1}{S}} \left(\theta_0 \hat{s}_t + \theta_1 x_t + \theta_2 x_{t-1} + \varepsilon_{s,t} + \left(\frac{1}{S} - 1 \right) \varepsilon_{c,t+1} \right), \quad (\text{A9})$$

$$\approx c_{t+1} - \varepsilon_{c,t+1} + \theta_0 (h_t - c_t) - \frac{\theta_1}{\frac{1}{S} - 1} x_t - \frac{\theta_2}{\frac{1}{S} - 1} x_{t-1} - \frac{1}{\frac{1}{S} - 1} \varepsilon_{s,t}, \quad (\text{A10})$$

$$\approx \theta_0 h_t + (1 - \theta_0) c_t + E_t \Delta c_{t+1} - \frac{\theta_1 x_t + \theta_2 x_{t-1}}{\frac{1}{S} - 1} - \frac{1}{\frac{1}{S} - 1} \varepsilon_{s,t}, \quad (\text{A11})$$

where we use $\Delta c_{t+1} = c_{t+1} - c_t$ to denote the change in log consumption from time t to time $t + 1$. We now iterate (A11) to obtain:

$$h_{t+1} \approx \sum_{j=0}^{\infty} \theta_0^j \left((1 - \theta_0) c_{t-j} + E_{t-j} \Delta c_{t-j+1} - \frac{1}{\frac{1}{S} - 1} \varepsilon_{s,t-j} - \frac{\theta_1 x_{t-j} + \theta_2 x_{t-j-1}}{\frac{1}{S} - 1} \right) \quad (\text{A12})$$

$$\approx (1 - \theta_0) \sum_{j=0}^{\infty} \theta_0^j c_{t-j} + \sum_{j=0}^{\infty} \theta_0^j E_{t-j} \Delta c_{t-j+1} - \frac{1}{\frac{1}{S} - 1} \sum_{j=0}^{\infty} \theta_0^j \varepsilon_{s,t-j} - \frac{\theta_1}{\frac{1}{S} - 1} x_t \quad (\text{A13})$$

$$- \frac{\theta_0 \theta_1 + \theta_2}{\frac{1}{S} - 1} \sum_{j=0}^{\infty} \theta_0^j x_{t-j-1}. \quad (\text{A14})$$

The expansion (A14) shows that approximate log habit depends on lagged moments of consumption, the output gap, and the habit shock. The resource constraint implies that output equals consumption, so the output gap equals the deviation of log consumption relative to a frictionless level.

In order to understand the compounded dependence of habit on the first and second lags of consumption, we substitute in for x_t from equation (20) in the main paper:

$$h_{t+1} \approx (1 - \theta_0) \sum_{j=0}^{\infty} \theta_0^j c_{t-j} + \sum_{j=0}^{\infty} \theta_0^j E_{t-j} \Delta c_{t-j+1} - \frac{1}{\frac{1}{S} - 1} \sum_{j=0}^{\infty} \theta_0^j \varepsilon_{s,t-j} \quad (\text{A15})$$

$$- \frac{\theta_1}{\frac{1}{S} - 1} \left(c_t - (1 - \phi) \sum_{i=0}^{\infty} \phi^i c_{t-1-i} - \sum_{i=0}^{\infty} \phi^i \Delta a_{t-i} \right) \quad (\text{A16})$$

$$- \frac{\theta_0 \theta_1 + \theta_2}{\frac{1}{S} - 1} \sum_{j=0}^{\infty} \theta_0^j \left(c_{t-j-1} - (1 - \phi) \sum_{i=0}^{\infty} \phi^i c_{t-j-2-i} - \sum_{i=0}^{\infty} \phi^i \Delta a_{t-i-1} \right). \quad (\text{A17})$$

The [Campbell and Cochrane \(1999\)](#) case corresponds to $\theta_1 = \theta_2 = 0$ and constant expected consumption growth. In that case, expression (A17) shows that log habit is approximately an exponentially-weighted moving average of lagged log consumption with exponential parameter θ_0 .

Our estimated model has $\theta_1 < 0$ and $\theta_2 > 0$, which allows us to generate hump-shaped output responses to monetary policy shocks that have been documented in macroeconomic data. Because $\frac{1}{\frac{1}{S} - 1} > 0$ and $1 - \phi$ is close to zero, a negative value for θ_1 raises the sensitivity of habit to the first two lags of consumption, while a positive value for θ_2 lowers the sensitivity of habit with respect to the second lag of consumption. Our model

uses $-\theta_1 > 0$, and $\theta_1(1 - \phi) - (\theta_0\theta_1 + \theta_2) = 0$ (which is the condition ensuring that the forward- and backward-looking coefficients in the log-linear macro Euler equation sum to one). Equation (A17) then implies that habit loads more on the first lag of consumption than in the Campbell-Cochrane case, but the loading onto the second consumption lag is unchanged.

B Proof of Phillips Curve

The derivation of the log-linearized Phillips curve is tedious, but almost all the steps in our derivation are standard. Our asset pricing habit preferences potentially enter in two places. This section shows that the log-linearized Phillips curve is invariant to both of these channels for the following two reasons:

1. Firms' real marginal cost depends on the real wage, which depends on preferences. The log-linearized Phillips curve is invariant to this channel, because we separate the intertemporal consumption-savings decision and the intratemporal labor-leisure choice as in Greenwood, Hercowitz, and Huffman (1988). We therefore obtain a standard functional form for log-linearized real marginal cost that does not depend on habit or surplus consumption.
2. The SDF enters into firms' first-order condition for the optimal price-setting decision. The log-linearized Phillips curve is invariant to this channel, because up to first-order our SDF is standard and second-order terms drop out of the log-linearized first-order condition, leading to a standard log-linearized Phillips curve.

We log linearize inflation around its random walk component v_t^* and output and labor around the steady-state with $\bar{Y}_t = A_t \bar{L}^{1-\tau}$ and \bar{L} the labor supply consistent with steady-state markups when prices are flexible. We use bars to denote steady-state values and hats to denote log deviations from this steady-state. We use lower-case letters to denote logs.

B.1 Marginal Cost of Production and Steady-State

In this section, we follow standard log-linearization steps to show that to first order firm i ' log deviation of marginal cost from steady-state takes the form:

$$\hat{m}c_{i,t} = a_0 \hat{y}_t - a_1 (p_{i,t} - p_t), \quad (\text{A18})$$

i.e. it increases in the log deviation of output from the steady state, and decreases in the log own-firm price deviation from the log aggregate price level where both a_0 and a_1 are positive constants. We use hats to denote log deviations from the steady-state, so that $\hat{y}_t = x_t$ is the log output gap.

We start from the household's labor-leisure condition. The household's period budget constraint takes the form

$$C_t + B_t \exp(-r_t) \leq B_{t-1} + \int_{i=0}^1 W_{i,t} L_{i,t} di + T_t. \quad (\text{A19})$$

Here, C_t is the Dixit-Stiglitz index of the aggregate consumption good, and P_t is the corresponding price. B_t represents purchases of the one-period real risk-free bond at price $\exp(-r_t)$, B_{t-1} is the quantity of the real risk-free government bond held from last period, $W_{i,t}L_{i,t}$ is the period t real wage income from providing labor of type i , and T_t is a real lump-sum component of income, which may include dividend ownership of firms, as well as taxes and transfers. Taking the first-order condition of household utility with respect to $L_{i,t}$ then gives the following condition for the real wage, $W_{i,t}$:

$$W_{i,t} = \frac{\frac{\partial U}{\partial L_{i,t}}}{\frac{\partial U}{\partial C_t}} = A_t N_t (1 - L_{i,t})^{-\chi}. \quad (\text{A20})$$

Firm i 's cost of producing quantity $Y_{i,t}$ of good i equals:

$$\text{Cost}_{i,t} = W_{i,t} L_{i,t} \quad (\text{A21})$$

$$= W_{i,t} \left(\frac{Y_{i,t}}{A_t N_t} \right)^{1/(1-\tau)} \quad (\text{A22})$$

Taking the derivative with respect to $Y_{i,t}$ and substituting in for the wage from (A20) gives the marginal cost of supplying good i :

$$MC_{i,t} = \frac{1}{1-\tau} \frac{W_{i,t}}{A_t N_t} \left(\frac{Y_{i,t}}{A_t N_t} \right)^{\frac{\tau}{1-\tau}}, \quad (\text{A23})$$

$$= \frac{1}{1-\tau} \left(1 - \left(\frac{Y_{i,t}}{A_t N_t} \right)^{1/(1-\tau)} \right)^{-\chi} \left(\frac{Y_{i,t}}{A_t N_t} \right)^{\frac{\tau}{1-\tau}}. \quad (\text{A24})$$

Note that here we have assumed that the producer is a wage taker following Woodford (2003, p.148). We define the steady-state labor supply \bar{L} to be the amount of labor supplied if markups are equal to the steady-state value $\bar{\mu} = \frac{\theta}{1-\theta}$, and all firms charge the same price. From (A24), \bar{L} is the solution of

$$\bar{\mu}^{-1} = \frac{1}{1-\tau} (1 - \bar{L})^{-\chi} \bar{L}^{\frac{\tau}{1-\tau}}. \quad (\text{A25})$$

We log-linearize around steady-state output, \bar{Y}_t :

$$\bar{Y}_t = A_t N_t \bar{L}^{1-\tau}. \quad (\text{A26})$$

At this steady-state the real wage for labor of type i equals

$$\bar{W}_{i,t} = A_t N_t (1 - \bar{L})^{-\chi}. \quad (\text{A27})$$

Log-linearizing the real wage around the steady-state wage gives:

$$\hat{w}_{i,t} = \chi \frac{\bar{L}}{1 - \bar{L}} \hat{l}_{i,t}, \quad (\text{A28})$$

$$= \eta \hat{l}_{i,t}. \quad (\text{A29})$$

Here, $\eta \equiv \chi_{\frac{\bar{L}}{1-\bar{L}}}$ is the inverse of the steady-state Frisch elasticity of labor supply.

Intermediate firm i 's elasticity of real marginal cost with respect to own-firm output near the steady-state then equals:

$$\frac{dMC_{i,t}}{dY_{i,t}} \frac{Y_{i,t}}{MC_{i,t}} = \frac{\tau}{1-\tau} + \frac{\eta}{1-\tau}, \quad (\text{A30})$$

$$\equiv \omega. \quad (\text{A31})$$

To first order, firm i 's log marginal cost relative to steady-state then equals

$$\begin{aligned} \widehat{mc}_{i,t} &= \log(MC_{i,t}) - \log(\bar{\mu}^{-1}), \\ &= \omega \hat{y}_{i,t}, \end{aligned} \quad (\text{A32})$$

$$= \omega \hat{y}_t - \omega \theta (p_{i,t} - p_t), \quad (\text{A33})$$

In the last step, we have used the demand function (11), log-linearized around the steady-state elasticity of substitution θ . We hence obtain the functional form (A18) with $a_0 = \omega$ and $a_1 = \omega\theta$.

We can compare (A33) to the log real marginal cost obtained with standard preferences (e.g. Woodford, 2003), where the real wage is given by

$$W_t = \frac{L_{i,t}^\eta}{C_t^{1-\gamma}}, \quad (\text{A34})$$

where η is the inverse of the Frisch elasticity of labor supply and γ is risk aversion. This expression is log-linearized to

$$\hat{w}_{i,t} = \gamma \hat{y}_t + \eta \hat{l}_{i,t}. \quad (\text{A35})$$

If instead, the log-linearized real wage took the form (A35), we would obtain the following log-linearized expression for the real marginal cost:

$$\widehat{mc}_{i,t} = (\omega + \gamma) \hat{y}_t - \omega \theta (p_{i,t} - p_t), \quad (\text{A36})$$

i.e. $a_0 = \omega + \gamma$ and $a_1 = \omega\theta$. Comparing expressions (A33) and (A36) shows that the log-linearized real wage in our model takes the same functional form as under standard preferences.

B.2 Discount Factor for Phillips Curve

We now derive the first-order approximation of the stochastic discount factor. Let $M_{t,t+j} = M_{t+1}M_{t+2}\dots M_{t+j}$ denote the household SDF for discounting cash flows at time $t+j$ back to time t . In the steady-state, log consumption grows at rate g and s_t is constant at \bar{s} . The steady-state SDF for discounting time $t+j$ real cash flows at time t takes the standard form:

$$\bar{M}_{t,t+j} = \beta^j \exp(-\gamma g j). \quad (\text{A37})$$

We denote log deviation of the SDF from this steady-state:

$$\hat{m}_{t,t+j} = \log \left(M_{t,t+j} / \bar{M}_{t,t+j} \right). \quad (\text{A38})$$

We will see that $\hat{m}_{t,t+j}$ drops out of the log-linearized price-setting first-order condition.

B.3 Price Level Law of Motion

The remainder of the derivation of the log-linearized profit first-order condition is standard and follows [Walsh \(2017\)](#). Because we have a unit root in inflation, we follow [Cogley and Sbordone \(2008\)](#) and log-linearize inflation around its random-walk trend v_t^* . Log deviations in inflation from its random walk trend are denoted by

$$\hat{\pi}_t = \pi_t - v_t^*, \quad (\text{A39})$$

and we log-linearize around $\hat{\pi}_t = 0$.

Since the probability of being able to adjust the price-level is independent and equal across firms, each firm that has the chance to re-set its price at time t chooses the same price \tilde{P}_t . The law of motion for the price level is

$$P_t^{-(\theta_t-1)} = \alpha \left(P_{t-1} \frac{P_{t-1}}{P_{t-2}} \right)^{-(\theta_t-1)} + (1-\alpha) \tilde{P}_t^{-(\theta_t-1)}. \quad (\text{A40})$$

Dividing [\(A40\)](#) by $P_t^{-(\theta_t-1)}$ gives

$$1 = \alpha \exp((\theta_t - 1) (\hat{\pi}_t - \hat{\pi}_{t-1} + v_{LT,t})) + (1 - \alpha) \left(\frac{\tilde{P}_t}{P_t} \right)^{-(\theta_t-1)}. \quad (\text{A41})$$

Using the notation $\tilde{p}_t = \log \left(\frac{\tilde{P}_t}{P_t} \right)$, to first-order the price-level law of motion is

$$\tilde{p}_t = \frac{\alpha}{1-\alpha} (\hat{\pi}_t - \hat{\pi}_{t-1} + v_{LT,t}). \quad (\text{A42})$$

B.4 Price-Setting First-Order Condition

The price charged at time $t+j$ by a firm that last got to reset its price at time t equals

$$\tilde{P}_t (P_{t-1+j} / P_{t-1}). \quad (\text{A43})$$

A firm that has the opportunity to re-set prices at time t chooses the price \tilde{P}_t to maximize the expected discounted sum of real profits conditional on the price still being in place:

$$\max_{\tilde{P}_t} E_t \sum_{j=0}^{\infty} \alpha^j M_{t,t+j} Y_{t+j} \left(\left(\frac{\tilde{P}_t P_{t-1+j} / P_{t-1}}{P_t P_{t+j} / P_t} \right)^{1-\theta_{t+j}} - \frac{Cost_{i,t+j}}{Y_{t+j}} \right). \quad (\text{A44})$$

The first-order condition with respect to the optimal price \tilde{P}_t equates the expected discounted sum of the marginal change in revenue with the expected discounted sum of the

marginal change in cost of producing the quantity demanded

$$\begin{aligned} & \frac{\tilde{P}_t}{P_t} E_t \sum_{j=0}^{\infty} \alpha^j M_{t,t+j} Y_{t+j} (\theta_{t+j} - 1) \left(\frac{P_{t-1+j}/P_{t-1}}{P_{t+j}/P_t} \right)^{1-\theta_{t+j}} \\ &= E_t \sum_{j=0}^{\infty} \alpha^j M_{t,t+j} Y_{t+j} \theta_{t+j} \left(\frac{P_{t-1+j}/P_{t-1}}{P_{t+j}/P_t} \right)^{-\theta_{t+j}} MC_{i,t+j}. \end{aligned} \quad (\text{A45})$$

B.5 Log-Linearizing the Profit First-Order Condition

We now log-linearize the first-order condition (A45) following the steps outlined in Walsh (2017), Chapter 8.7. In the flexible-price equilibrium with θ_t at its steady-state value θ , all firms charge the same price so $\overline{MC} = \bar{\mu}^{-1} = \frac{\theta-1}{\theta}$. Denoting the log of steady-state output by $\bar{y}_t \equiv \log \bar{Y}_t$ we have that

$$\bar{y}_{t+1} - \bar{y}_t = \Delta n_{t+1} + \Delta a_{t+1}, \quad (\text{A46})$$

$$= \nu + (1 - \phi)(1 - \tau)l_t + \Delta a_{t+1}, \quad (\text{A47})$$

$$= g + (1 - \phi)\hat{y}_t + \Delta a_{t+1}, \quad (\text{A48})$$

where the steady-state growth rate, g , equals

$$g = \nu + (1 - \phi)(1 - \tau)\bar{l}. \quad (\text{A49})$$

To save on notation, we define:

$$\beta_g = \beta \exp(-(\gamma - 1)g). \quad (\text{A50})$$

The log-linear expansion for the left-hand-side of (A45) conditional on \bar{Y}_t becomes:

$$\begin{aligned} & (1 + \tilde{p}_t) E_t \sum_{j=0}^{\infty} \left[(\beta_g \alpha)^j \bar{Y}_t (1 + \hat{y}_{t+j}) (1 + (\bar{y}_{t+j} - \bar{y}_t - g)) (1 + \hat{m}_{t,t+j}) (\theta(1 + \hat{\theta}_{t+j}) - 1) \times \right. \\ & \left. (1 + (1 - \theta(1 + \hat{\theta}_{t+j}))) (\hat{\pi}_t - \hat{\pi}_{t+j} + (v_{t+1}^{LT} + \dots + v_{t+j}^{LT})) \right]. \end{aligned} \quad (\text{A51})$$

Dropping second-order terms and collecting terms that are independent of j gives

$$\begin{aligned} & \frac{\bar{Y}_t(\theta - 1)}{1 - \beta_g \alpha} + \frac{\bar{Y}_t \tilde{p}_t(\theta - 1)}{1 - \beta_g \alpha} \\ & + \bar{Y}_t(\theta - 1) E_t \sum_{j=0}^{\infty} (\beta_g \alpha)^j \left(\hat{y}_{t+j} + (\bar{y}_{t+j} - \bar{y}_t - g) + \hat{m}_{t,t+j} + \bar{\mu} \hat{\theta}_{t+j} + (1 - \theta)(\hat{\pi}_t - \hat{\pi}_{t+j}) \right). \end{aligned} \quad (\text{A52})$$

Next, we approximate the right-hand-side of (A45) log-linearly. This gives

$$E_t \sum_{j=0}^{\infty} \left[(\beta_g \alpha)^j \bar{Y}_t (1 + \hat{y}_{t+j}) (1 + (\bar{y}_{t+j} - \bar{y}_t - g)) (1 + \hat{m}_{t,t+j}) \theta (1 + \hat{\theta}_{t+j}) \times \right. \\ \left. \left(1 - \theta (1 + \hat{\theta}_{t+j}) (\hat{\pi}_t - \hat{\pi}_{t+j} + (v_{t+1}^{LT} + \dots + v_{t+j}^{LT})) \right) \overline{MC} (1 + \widehat{mc}_{t+j}) \right]. \quad (\text{A53})$$

Next, we use $\theta \overline{MC} = \theta - 1$, note that $E_t v_{t+k}^{LT} = 0$ for $k > 0$, substitute in (A33), and drop second-order terms:

$$\begin{aligned} & \frac{\bar{Y}_t(\theta - 1)}{1 - \beta_g \alpha} + \bar{Y}_t(\theta - 1) E_t \sum_{j=0}^{\infty} (\beta_g \alpha)^j \left(\hat{y}_{t+j} + (\bar{y}_{t+j} - \bar{y}_t - g) + \hat{m}_{t,t+j} + \hat{\theta}_{t+j} \right) \\ & + \bar{Y}_t(\theta - 1) E_t \sum_{j=0}^{\infty} (\beta_g \alpha)^j \left(-\theta (\hat{\pi}_t - \hat{\pi}_{t+j}) + \widehat{mc}_{t+j} \right), \quad (\text{A54}) \\ = & \frac{\bar{Y}_t(\theta - 1)}{1 - \beta_g \alpha} + \bar{Y}_t(\theta - 1) E_t \sum_{j=0}^{\infty} (\beta_g \alpha)^j \left(\hat{y}_{t+j} + (\bar{y}_{t+j} - \bar{y}_t - g) + \hat{m}_{t,t+j} + \hat{\theta}_{t+j} \right) \\ & + \bar{Y}_t(\theta - 1) E_t \sum_{j=0}^{\infty} (\beta_g \alpha)^j \left(-\theta (\hat{\pi}_t - \hat{\pi}_{t+j}) + a_0 \hat{y}_{t+j} \right) \\ & - a_1 \left(\frac{\bar{Y}_t(\theta - 1) \tilde{p}_t}{1 - \beta_g \alpha} + \bar{Y}_t(\theta - 1) E_t \sum_{j=0}^{\infty} (\beta_g \alpha)^j (\hat{\pi}_t - \hat{\pi}_{t+j}) \right). \quad (\text{A55}) \end{aligned}$$

Equating (A52) and (A55), cancelling common terms, and dividing by $\bar{Y}_t(\theta - 1)$ gives

$$\begin{aligned} & (1 + a_1) \left(\frac{\tilde{p}_t}{1 - \beta_g \alpha} + \frac{\hat{\pi}_t}{1 - \beta_g \alpha} - E_t \sum_{j=0}^{\infty} (\beta_g \alpha)^j \hat{\pi}_{t+j} \right) \\ = & E_t \sum_{j=0}^{\infty} (\beta_g \alpha)^j (a_0 \hat{y}_{t+j} + \hat{\mu}_{t+j}), \quad (\text{A56}) \end{aligned}$$

where the log deviation of the markup from steady-state is given by

$$\hat{\mu}_{t+j} = \frac{d\mu_{t+j}}{d\theta_{t+j}} \frac{\mu_{t+j}}{\theta_{t+j}} \hat{\theta}_{t+j} = \frac{1}{\theta - 1} \hat{\theta}_{t+j} = (1 - \bar{\mu}) \hat{\theta}_{t+j}. \quad (\text{A57})$$

Note in particular that $\hat{m}_{t,t+j}$ drops out of (A56). Because this is the main place where we differ from the standard New Keynesian model, this makes clear that our asset pricing preferences drop out of the log-linearized optimal price-setting decision.

B.6 Substituting out \tilde{p}_t

Next, we follow a number of standard steps (e.g. Walsh (2017)) to solve for $\hat{\pi}_t$. From equation (A56) we have:

$$\begin{aligned}
\tilde{p}_t + \hat{\pi}_t &= (1 - \beta_g \alpha) E_t \sum_{j=0}^{\infty} (\beta_g \alpha)^j \left(\frac{a_0 \hat{y}_{t+j} + \hat{\mu}_{t+j}}{1 + a_1} + \hat{\pi}_{t+j} \right), \quad (\text{A58}) \\
&= \frac{1 - \beta_g \alpha}{1 + a_1} (a_0 \hat{y}_t + \hat{\mu}_t) + (1 - \beta_g \alpha) \hat{\pi}_t \\
&\quad + \beta_g \alpha (1 - \beta_g \alpha) E_t \sum_{j=0}^{\infty} (\beta_g \alpha)^j \left(\frac{a_0 \hat{y}_{t+1+j} + \hat{\mu}_{t+1+j}}{1 + a_1} + \hat{\pi}_{t+1+j} \right), \\
&= \frac{1 - \beta_g \alpha}{1 + a_1} (a_0 \hat{y}_t + \hat{\mu}_t) + (1 - \beta_g \alpha) \hat{\pi}_t + \beta_g \alpha E_t (\tilde{p}_{t+1} + \hat{\pi}_{t+1}) \quad (\text{A59})
\end{aligned}$$

This equation relates the optimal relative price to the current-period marginal cost, current-period optimal markup, and the next-period expected optimal relative price. Subtracting $\hat{\pi}_t$ from both sides gives

$$\tilde{p}_t = \frac{1 - \beta_g \alpha}{1 + a_1} (a_0 \hat{y}_t + \hat{\mu}_t) - \beta_g \alpha \hat{\pi}_t + \beta_g \alpha E_t \hat{\pi}_{t+1} + \beta_g \alpha E_t \tilde{p}_{t+1}. \quad (\text{A60})$$

Substituting in the log-linearized law of motion for inflation (A42) and multiplying by $\frac{1-\alpha}{\alpha}$ gives

$$\left(\hat{\pi}_t - \hat{\pi}_{t-1} + v_t^{LT} \right) = \frac{1 - \alpha}{\alpha} \frac{1 - \beta_g \alpha}{1 + a_1} (a_0 \hat{y}_t + \hat{\mu}_t) - \beta_g \hat{\pi}_t + \beta_g E_t \hat{\pi}_{t+1} \quad (\text{A61})$$

Solving for $\hat{\pi}_t$ gives the New Keynesian Phillips Curve (ignoring constants)

$$\hat{\pi}_t = \frac{\beta_g}{1 + \beta_g} E_t \hat{\pi}_{t+1} + \frac{1}{1 + \beta_g} \hat{\pi}_{t-1} + \kappa \hat{y}_t + \frac{\kappa}{a_0} \hat{\mu}_t - \frac{1}{1 + \beta_g} v_t^{LT}, \quad (\text{A62})$$

where the Phillips curve slope coefficient on \hat{y}_t equals

$$\kappa = \frac{1}{1 + \beta_g} \frac{1 - \alpha}{\alpha} (1 - \beta_g \alpha) \frac{a_0}{1 + a_1}. \quad (\text{A63})$$

Finally, we use that (up to a constant)

$$\hat{\mu}_t = \frac{1}{1 - \theta} \varepsilon_{\theta,t} \quad (\text{A64})$$

$$x_t = \hat{y}_t, \quad (\text{A65})$$

$$a_0 = \omega, \quad (\text{A66})$$

$$a_1 = \omega \theta, \quad (\text{A67})$$

and add the unit root component v_t^* to both sides of (A62) to obtain the log-linearized New Keynesian Phillips curve (30) in the main paper.

Note that the Phillips curve slope κ is identical to Woodford(1999, p.342) with three

exceptions. First, β is replaced by β_g because we have equilibrium growth in our model. Second, the factor $\frac{1}{1+\beta_g}$ is new. This is due to indexing. Third, $a_0 = \omega$, whereas in Woodford (2003) the sensitivity of marginal cost with respect to aggregate log output is $\omega + \gamma$. This is due to our separation between the intertemporal consumption-savings trade-off and the intratemporal labor-leisure trade-off as in Greenwood, Hercowitz, and Huffman (1988). However, (Woodford (2003, p.341)) estimates a very small value for the curvature parameter from macroeconomic data of $\gamma = 0.16$, so the log-linearized Phillips curve in our model is not only qualitatively but also quantitatively in line with this prior work.

C Model Solution

C.1 Output gap and consumption relationships

With the assumption on the evolution of human capital (15), we can iterate to obtain

$$n_t = \nu + n_{t-1} + (1 - \phi)(1 - \tau)l_{t-1}, \quad (\text{A68})$$

$$= \nu + n_{t-1} + (1 - \phi)(y_{t-1} - a_{t-1}), \quad (\text{A69})$$

$$= \frac{\nu}{1 - \phi} + (1 - \phi) \sum_{j=0}^{\infty} \phi^j (y_{t-1-j} - a_{t-1-j}). \quad (\text{A70})$$

The deviation of output from the flexible-price equilibrium then equals (up to a constant):

$$x_t = y_t - n_t - a_t, \quad (\text{A71})$$

$$= y_t - (1 - \phi) \sum_{j=0}^{\infty} \phi^j (y_{t-1-j} - a_{t-1-j}) - a_t, \quad (\text{A72})$$

$$= c_t - (1 - \phi) \sum_{j=0}^{\infty} \phi^j c_{t-1-j} - \sum_{j=0}^{\infty} \phi^j \Delta a_{t-j}, \quad (\text{A73})$$

i.e. equation (20) in the main paper. Because Δa_t is stationary and the geometric series ϕ^j has a finite sum, the deviation between the output gap x_t and stochastically detrended consumption is stationary. Consumption growth then takes the following simple form (up to a constant):

$$\Delta c_{t+1} = (x_{t+1} + \sum_{j=0}^{\infty} \phi^j \Delta a_{t+1-j}) - \phi(x_t - \sum_{j=0}^{\infty} \phi^j \Delta a_{t-j}), \quad (\text{A74})$$

$$= x_{t+1} - \phi x_t + \Delta a_{t+1}, \quad (\text{A75})$$

i.e. equation (21) in the main paper.

C.2 Deriving the macro Euler equation

With the updating equation for log consumption growth (A75), the asset pricing Euler equation for the one-period real risk-free rate is given by:

$$r_t = \gamma E_t \Delta c_{t+1} + \gamma E_t \Delta \hat{s}_{t+1} - \frac{\gamma^2}{2} (1 + \lambda(s_t))^2 \sigma_c^2, \quad (\text{A76})$$

$$= \gamma E_t \Delta c_{t+1} + \gamma(\theta_0 - 1)\hat{s}_t + \gamma\theta_1 x_t + \gamma\theta_2 x_{t-1} + \gamma\varepsilon_{s,t} - \frac{\gamma^2}{2} (1 + \lambda(s_t))^2 \sigma_c^2, \quad (\text{A77})$$

$$= \gamma \Delta a_{t+1} + \gamma E_t x_{t+1} - \gamma \phi x_t + \gamma(\theta_0 - 1)\hat{s}_t + \gamma\theta_1 x_t + \gamma\theta_2 x_{t-1} + \gamma\varepsilon_{s,t} - \frac{\gamma^2}{2} (1 + \lambda(s_t))^2 \sigma_c^2$$

The sensitivity function has just the right form so that surplus consumption \hat{s}_t drops out and (up to a constant):

$$r_t = \gamma \Delta a_{t+1} + \gamma E_t x_{t+1} - \gamma \phi x_t + \gamma \theta_1 x_t + \gamma \theta_2 x_{t-1} + \gamma \varepsilon_{s,t} \quad (\text{A78})$$

Rearranging and continuing to ignore constants gives:

$$x_t = \frac{1}{\phi - \theta_1} E_t x_{t+1} + \frac{\theta_2}{\phi - \theta_1} x_{t-1} - \frac{1}{\gamma(\phi - \theta_1)} (r_t - \gamma \Delta a_{t+1}) + \frac{1}{\phi - \theta_1} \varepsilon_{s,t}. \quad (\text{A79})$$

Note that we have not made any approximations in the derivation of (26).

C.3 Solving for macroeconomic dynamics

We want to find a solution of the form

$$Y_t = B Y_{t-1} + \Sigma v_t, \quad (\text{A80})$$

where the matrix B is $[3 \times 3]$, the matrix Σ is $[3 \times 4]$, and the state vector Y_t is defined in equation (31) in the main paper. Throughout, we use Σ_v to denote the (diagonal) variance-covariance matrix of the vector of shocks, v_t . Substituting in for predictable productivity growth from equation (16) in main paper into (A79), We collect the log-linear equations describing the macroeconomic equilibrium dynamics:

$$x_t = f^x E_t x_{t+1} + \rho^x x_{t-1} - \psi (r_t - \gamma \rho^a r_t - \gamma \varepsilon_{s,t}), \quad (\text{A81})$$

$$\pi_t = f^\pi E_t \pi_{t+1} + \rho^\pi \pi_{t-1} + \kappa x_t + v_{\pi,t}, \quad (\text{A82})$$

$$i^* = \gamma^x x_t + \gamma^\pi \pi_t + (1 - \gamma^\pi) v_t^*, \quad (\text{A83})$$

$$i_t = \rho^i i_{t-1} + (1 - \rho^i) i_t^* + v_{ST,t}, \quad (\text{A84})$$

$$v_t^* = v_{t-1}^* + v_{LT,t} \quad (\text{A85})$$

Writing this in terms of the elements of Y_t and using that $v_{x,t} = \gamma\psi\varepsilon_{s,t}$ gives

$$Y_{1,t} = f^x E_t Y_{1,t+1} + \rho^x Y_{1,t-1} - \psi(1 - \gamma\rho^a)(Y_{3,t} - E_t Y_{2,t+1}) + v_{x,t}, \quad (\text{A86})$$

$$Y_{2,t} = f^\pi E_t Y_{2,t+1} + \rho^\pi Y_{2,t-1} + \kappa Y_{1,t} + v_{\pi,t} - \rho^\pi v_{LT,t}, \quad (\text{A87})$$

$$Y_{3,t} = \rho^i Y_{3,t-1} + (1 - \rho^i)(\gamma^x Y_{1,t} + \gamma^\pi Y_{2,t}) + v_{ST,t} - \rho^i v_{LT,t}, \quad (\text{A88})$$

$$v_t^* = v_{t-1}^* + v_{LT,t}. \quad (\text{A89})$$

The same thing in matrix form:

$$0 = FE_t Y_{t+1} + GY_t + HY_{t-1} + Mv_t,$$

where the matrices F , G and H are given by

$$F = \begin{bmatrix} f^x & \psi(1 - \gamma\rho^a) & 0 \\ 0 & f^\pi & 0 \\ 0 & 0 & 0 \end{bmatrix},$$

$$G = \begin{bmatrix} -1 & 0 & -\psi(1 - \gamma\rho^a) \\ \kappa & -1 & 0 \\ (1 - \rho^i)\gamma^x & (1 - \rho^i)\gamma^\pi & -1 \end{bmatrix},$$

$$H = \begin{bmatrix} \rho^x & 0 & 0 \\ 0 & \rho^\pi & 0 \\ 0 & 0 & \rho^i \end{bmatrix}.$$

The matrix M is $[3 \times 4]$ and equals:

$$M = \begin{bmatrix} 1 & 0 & 0 & 0 \\ 0 & 1 & 0 & -\rho^\pi \\ 0 & 0 & 1 & -\rho^i \end{bmatrix} \quad (\text{A90})$$

Following Uhlig (1999), we solve for the generalized eigenvectors and eigenvalues of the matrix Ξ with respect to the matrix Δ , where

$$\Xi = \begin{bmatrix} -G & -H \\ I_3 & 0_3 \end{bmatrix}, \quad (\text{A91})$$

$$\Delta = \begin{bmatrix} F & 0_3 \\ 0_3 & I_3 \end{bmatrix} \quad (\text{A92})$$

To obtain a solution, we then pick three generalized eigenvalues $\lambda_1, \lambda_2, \lambda_3$ with generalized eigenvectors $[\lambda z'_1, z'_1]'$, $[\lambda_2 z'_2, z'_2]'$, and $[\lambda_3 z'_3, z'_3]'$. We denote the diagonal matrix of these eigenvalues by $\Lambda = \text{diag}(\lambda_1, \lambda_2, \lambda_3)$, and the matrix of the lower $[3 \times 1]$ portion of the eigenvectors by $\Omega = [z_1, z_2, z_3]$. The corresponding solutions for B and Σ are then given by:

$$B = \Omega\Lambda\Omega^{-1}, \quad (\text{A93})$$

$$\Sigma = [FB + G]^{-1} M. \quad (\text{A94})$$

In our empirical application, there exist exactly three generalized eigenvalues with absolute value less than one, and we pick the non-explosive solution corresponding to these three eigenvalues.

C.4 Rotated state vector

Our state space for solving for asset prices is five-dimensional: It consists of \tilde{Z}_t , which is a scaled version of Y_t , the surplus consumption ratio relative to steady-state \hat{s}_t , and the lagged output gap x_{t-1} . The lagged output gap x_{t-1} is not actually needed as a state variable and we have verified that our numerical solutions for asset prices do not vary with x_{t-1} . Our code includes x_{t-1} as a state variable for legacy reasons.

We next describe the definition of \tilde{Z}_t . To simplify the numerical implementation of the asset pricing recursions, we require that shocks to the scaled state vector \tilde{Z}_t are independent standard normal and that the first dimension of the scaled state vector is perfectly correlated with output gap innovations. This rotation facilitates the numerical analysis, because it is easier to integrate over independent random variables. Aligning the first dimension of the scaled state vector with output gap innovations (and hence surplus consumption innovations) helps, because it allows us to use a finer grid to integrate numerically over this crucial dimension over which asset prices are most non-linear.

If the scaled state vector equals $\tilde{Z}_t = AY_t$ for some invertible matrix A , the dynamics of \tilde{Z}_t are given by:

$$\tilde{Z}_t = AY_t, \quad (\text{A95})$$

$$\tilde{Z}_{t+1} = \underbrace{ABA^{-1}}_{\tilde{B}} \tilde{Z}_t + \underbrace{A\Sigma v_{t+1}}_{\epsilon_{t+1}}. \quad (\text{A96})$$

We hence want a matrix, A , such that

$$\text{Var}(\epsilon_{t+1}) = A\Sigma\Sigma_v\Sigma' A', \quad (\text{A97})$$

$$= \begin{bmatrix} 1 & 0 & 0 \\ 0 & 1 & 0 \\ 0 & 0 & 1 \end{bmatrix}. \quad (\text{A98})$$

Finding such a matrix A should in general be possible, because the matrix M and therefore $\Sigma\Sigma_v\Sigma'$ hence generally have rank three. We require that the first dimension of ϵ_{t+1} is perfectly correlated with the consumption shock. We can therefore find the three rows of A using the following steps:

1. Set $A_1 = \frac{e_1}{\sqrt{e_1\Sigma\Sigma_v\Sigma'e_1}}$.
2. We use the MATLAB function *null* to compute the null space of $A_1\Sigma\Sigma_v\Sigma'$. Let n_2 denote the first vector in *null*($A_1\Sigma\Sigma_v\Sigma'$). We then define the second row of A as the normalized version of n_2 :

$$A_2 = \frac{n_2}{\sqrt{n_2\Sigma\Sigma_v\Sigma'n_2'}}$$
(A99)

3. Let n_3 denote the first vector in $\text{null}(A_1 \Sigma \Sigma_v \Sigma', A_2 \Sigma \Sigma_v \Sigma')$. We then define the third row of A as the normalized version of n_3 :

$$A_3 = \frac{n_3}{\sqrt{n_3 \Sigma \Sigma_v \Sigma' n_3}}. \quad (\text{A100})$$

It is then straightforward to verify that equation (A98) holds for

$$A = \begin{bmatrix} A_1 \\ A_2 \\ A_3 \end{bmatrix}. \quad (\text{A101})$$

C.5 Asset pricing recursions

Before deriving the recursions for the numerical asset pricing computations, we derive a convenient form for the dynamics of the log surplus consumption ratio. We use e_i to denote a row vector with 1 in position i and zeros elsewhere. The matrix

$$\Sigma_M = e_1 \Sigma \quad (\text{A102})$$

denotes the loading of consumption innovations onto the vector of shocks v_t , where e_1 is a basis vector with a one in the first position and zeros everywhere else. The volatility of consumption surprises equals:

$$\sigma_c^2 = \Sigma_M \Sigma_v \Sigma_M'. \quad (\text{A103})$$

To simplify notation, we define \hat{s}_t as the log deviation of surplus consumption from its steady state. The dynamics of \hat{s}_t are:

$$\hat{s}_t = s_t - \bar{s}, \quad (\text{A104})$$

$$\hat{s}_t = \theta_0 \hat{s}_{t-1} + \theta_1 x_{t-1} + \theta_2 x_{t-2} + \varepsilon_{s,t-1} + \lambda(\hat{s}_{t-1}) \varepsilon_{c,t}, \quad (\text{A105})$$

where with an abuse of notation we write:

$$\lambda(\hat{s}_t) = \lambda_0 \sqrt{1 - 2\hat{s}_t - 1}, \hat{s}_t \leq s_{max} - \bar{s}, \quad (\text{A106})$$

$$\lambda(\hat{s}_t) = 0, \hat{s}_t \geq s_{max} - \bar{s}. \quad (\text{A107})$$

The steady-state surplus consumption sensitivity equals:

$$\lambda_0 = \frac{1}{\bar{S}}. \quad (\text{A108})$$

In our calculations of asset prices, we repeatedly substitute out expected log SDF growth, which equals:

$$E_t[m_{t+1}] = \log \beta - \gamma E_t \Delta \hat{s}_{t+1} - \gamma E_t \Delta c_{t+1}, \quad (\text{A109})$$

$$= -r_t - \frac{\gamma}{2} (1 - \theta_0) (1 - 2\hat{s}_t). \quad (\text{A110})$$

We often combine this with $r_t = \bar{r} + (e_3 - e_2 B)Z_t$ and $\hat{r}_t = (e_3 - e_2 B)Z_t$.

Including the constant, consumption growth is given by:

$$\Delta c_{t+1} = g + x_{t+1} - \phi x_t + \Delta a_{t+1}, \quad (\text{A111})$$

$$= g + x_{t+1} - \phi x_t + \rho^a \hat{r}_t. \quad (\text{A112})$$

The steady state real short-term interest rate at $x_t = 0$ and $s_t = \bar{s}$ is the same as in [Campbell and Cochrane \(1999\)](#):

$$\bar{r} = \gamma g - \frac{1}{2} \gamma^2 \sigma_c^2 / \bar{S}^2 - \log(\beta). \quad (\text{A113})$$

The updating rule for the log surplus consumption ratio can then be written in terms of the state variables as:

$$\hat{s}_{t+1} = \hat{s}_t + E_t \Delta \hat{s}_{t+1} + \lambda(\hat{s}_t) \varepsilon_{c,t+1}, \quad (\text{A114})$$

$$= \hat{s}_t - E_t \Delta \hat{c}_{t+1} + \frac{1}{\gamma} \left(\log \beta + \hat{r}_t + \bar{r} + \frac{\gamma}{2} (1 - \theta_0) (1 - 2\hat{s}_t) \right) + \lambda(\hat{s}_t) \varepsilon_{c,t+1}, \quad (\text{A115})$$

$$= \theta_0 \hat{s}_t + \frac{1}{\gamma} (e_3 - e_2 B) A^{-1} \tilde{Z}_t - e_1 [B - \phi I] A^{-1} \tilde{Z}_t - \rho^a \hat{r}_t + \lambda(\hat{s}_t) \varepsilon_{c,t+1}, \quad (\text{A116})$$

$$= \theta_0 \hat{s}_t + \frac{1}{\gamma} (1 - \gamma \rho^a) (e_3 - e_2 B) A^{-1} \tilde{Z}_t - e_1 [B - \phi I] A^{-1} \tilde{Z}_t + \lambda(\hat{s}_t) \varepsilon_{c,t+1}. \quad (\text{A117})$$

C.5.1 Recursion for zero-coupon consumption claims

We now derive the recursion for zero-coupon consumption claims in terms of state variables \tilde{Z}_t , \hat{s}_t and x_{t-1} . Let P_{nt}^c/C_t denote the price-dividend ratio of a zero-coupon claim on consumption at time $t+n$. The outline of our strategy here is that we first derive an analytic expression for the price-dividend ratio for P_{1t}^c/C_t . For $n \geq 1$ we guess and verify recursively that there exists a function $F_n(\tilde{Z}_t, \hat{s}_t, x_{t-1})$, such that

$$\frac{P_{nt}^c}{C_t} = F_n(\tilde{Z}_t, \hat{s}_t, x_{t-1}). \quad (\text{A118})$$

The ex-dividend price-consumption ratio for a claim to all future consumption is then given by

$$\frac{P_t}{C_t} = F(\tilde{Z}_t, \hat{s}_t, x_{t-1}), \quad (\text{A119})$$

where we define

$$F(\tilde{Z}_t, \hat{s}_t, x_{t-1}) = \sum_{n=1}^{\infty} F_n(\tilde{Z}_t, \hat{s}_t, x_{t-1}). \quad (\text{A120})$$

We now derive the recursion of zero-coupon consumption claims in terms of state variables \tilde{Z}_t and \hat{s}_t . The one-period zero coupon price-consumption ratio solves:

$$\frac{P_{1,t}^c}{C_t} = E_t \left[\frac{M_{t+1} C_{t+1}}{C_t} \right] \quad (\text{A121})$$

We simplify

$$\frac{M_{t+1}C_{t+1}}{C_t} = \beta \exp(E_t m_{t+1} + E_t \Delta c_{t+1} - \gamma(\hat{s}_{t+1} - E_t s_{t+1}) - (\gamma - 1)(c_{t+1} - E_t c_{t+1})).$$

Using the notation $f_n = \log(F_n)$, this gives the log one-period price-consumption ratio as:

$$\begin{aligned} f_1(\tilde{Z}_t, \hat{s}_t, x_{t-1}) &= -r_t - \frac{\gamma}{2}(1 - \theta_0)(1 - 2\hat{s}_t) + g + \Delta a_{t+1} + E_t x_{t+1} - \phi x_t \\ &\quad + \frac{1}{2}(\gamma\lambda(\hat{s}_t) + (\gamma - 1))^2 \sigma_c^2, \end{aligned} \quad (\text{A122})$$

$$\begin{aligned} &= g + e_1 [B - \phi I] A^{-1} \tilde{Z}_t + \frac{1}{2}(\gamma\lambda(\hat{s}_t) + (\gamma - 1))^2 \sigma_c^2 \\ &\quad - \bar{r} - (1 - \rho^a)(e_3 - e_2 B) A^{-1} \tilde{Z}_t - \frac{\gamma}{2}(1 - \theta_0)(1 - 2\hat{s}_t) \end{aligned} \quad (\text{A123})$$

Next, we solve for f_n , $n \geq 2$ iteratively. Note that:

$$\frac{P_{nt}^c}{C_t} = \mathbb{E}_t \left[\frac{M_{t+1}C_{t+1}}{C_t} \frac{P_{n-1,t+1}^c}{C_{t+1}} \right] = \mathbb{E}_t \left[\frac{M_{t+1}C_{t+1}}{C_t} F_{n-1}(\tilde{Z}_{t+1}, \hat{s}_{t+1}, x_t) \right] \quad (\text{A124})$$

This gives the following expression for f_n :

$$\begin{aligned} f_n(\tilde{Z}_t, \hat{s}_t, \hat{r}_{t-1}) &= \log \left[\mathbb{E}_t \left[\exp \left(g + e_1 [B - \phi I] A^{-1} \tilde{Z}_t \right. \right. \right. \\ &\quad \left. \left. - \bar{r} - (1 - \rho^a)(e_3 - e_2 B) A^{-1} \tilde{Z}_t - \frac{\gamma}{2}(1 - \theta_0)(1 - 2\hat{s}_t) \right. \right. \\ &\quad \left. \left. - (\gamma(1 + \lambda(\hat{s}_t)) - 1) \sigma_c \epsilon_{1,t+1} \right. \right. \\ &\quad \left. \left. + f_{n-1}(\tilde{Z}_{t+1}, \hat{s}_{t+1}, \hat{r}_t) \right) \right]. \end{aligned} \quad (\text{A125})$$

Here, $\epsilon_{1,t+1}$ denotes the first dimension of the shock ϵ_{t+1} .

C.5.2 Recursion for zero-coupon bond prices

We use $P_{n,t}^{\$}$ and $P_{n,t}$ to denote the prices of nominal and real n -period zero-coupon bonds. The strategy is to develop analytic expressions for one- and two-period bond prices. We then guess and verify recursively that the prices of real and nominal zero-coupon bonds with maturity $n \geq 2$ can be written in the following form:

$$P_{n,t} = B_n(\tilde{Z}_t, \hat{s}_t, x_{t-1}), \quad (\text{A126})$$

$$P_{n,t}^{\$} = \exp(-nv_t^*) B_n^{\$}(\tilde{Z}_t, \hat{s}_t, x_{t-1}), \quad (\text{A127})$$

where $B_n(\tilde{Z}_t, \hat{s}_t, x_{t-1})$ and $B_n^{\$}(\tilde{Z}_t, \hat{s}_t, x_{t-1})$ are functions of the state variables. As discussed in the main paper, we assume that the short-term nominal interest rate contains no risk premium, so the one-period log nominal interest rate equals $i_t = r_t + E_t \pi_{t+1}$. Taking account of the constants, one-period bond prices equal:

$$P_{1,t}^{\$} = \exp(-Y_{3,t} - v_t^* - \bar{r}), \quad (\text{A128})$$

$$P_{1,t} = \exp(-Y_{3,t} + \mathbb{E}_t Y_{2,t+1} - \bar{r}). \quad (\text{A129})$$

We next solve for longer-term bond prices including risk premia. Substituting in (A128) into the bond-pricing recursion gives:

$$P_{2,t}^{\$} = \mathbb{E}_t \left[M_{t+1} P_{1,t+1}^{\$} \exp(-v_{t+1}^* - Y_{2,t+1}) \right] \quad (\text{A130})$$

$$= \mathbb{E}_t \left[M_{t+1} \exp(-Y_{3,t+1} - 2v_{t+1}^* - Y_{2,t+1} - \bar{r}) \right]. \quad (\text{A131})$$

We can now verify that the two-period nominal bond price takes the form (A127):

$$\begin{aligned} B_2^{\$}(\tilde{Z}_t, \hat{s}_t, x_{t-1}) &= \exp(E_t(m_{t+1} - Y_{3,t+1} - Y_{2,t+1}) - \bar{r}) \\ &\times \mathbb{E}_t \left[\exp \left(\left(-\gamma(\lambda(\hat{s}_t) + 1) \Sigma_M - \underbrace{[(e_2 + e_3)\Sigma + 2e_4]}_{v_{\$}} \right) v_{t+1} \right) \right]. \end{aligned} \quad (\text{A132})$$

Here, we define the vector $v_{\$}$ to simplify notation. The random walk component of inflation v_t^* does not appear in (A132), because $B_2^{\$}$ is already scaled by $\exp(-2v_t^*)$ by definition (A127). Taking logs, substituting out for $E_t m_{t+1}$, and using the definition for the sensitivity function $\lambda(\hat{s}_t)$, we get:

$$\begin{aligned} b_2^{\$} &= -e_3[I + B]A^{-1}\tilde{Z}_t + \frac{1}{2}v_{\$}\Sigma_v v_{\$}' \\ &\quad + \gamma(\lambda(\hat{s}_t) + 1)\Sigma_M \Sigma_v v_{\$}' - 2\bar{r}. \end{aligned} \quad (\text{A133})$$

We similarly solve for two-period real bond prices in closed form:

$$\begin{aligned} P_{2,t} &= \exp(E_t(m_{t+1} - Y_{3,t+1} + Y_{2,t+2}) - \bar{r}) \\ &\times \mathbb{E}_t \left[\exp \left((-\gamma(\lambda(\hat{s}_t) + 1)\Sigma_M - \underbrace{(e_3 - e_2B)\Sigma}_{v_r}) v_{t+1} \right) \right] \end{aligned} \quad (\text{A134})$$

We define the vector v_r to simplify notation. Taking logs, substituting out for $E_t m_{t+1}$, and using the definition for $\lambda(\hat{s}_t)$ gives:

$$b_2(\tilde{Z}_t, \hat{s}_t, x_{t-1}) = -(e_3 - e_2B)[I + B]A^{-1}\tilde{Z}_t + \frac{1}{2}v_r \Sigma_v v_r' + \gamma(\lambda(\hat{s}_t) + 1)\Sigma_M \Sigma_v v_r' - 2\bar{r}. \quad (\text{A135})$$

For $n \geq 3$, we repeatedly substitute out for $E_t m_{t+1}$ to obtain the following recursion for real bond prices:

$$\begin{aligned} B_n(\tilde{Z}_t, \hat{s}_t, x_{t-1}) &= \mathbb{E}_t \left[\exp \left(m_{t+1} + b_{n-1}(\tilde{Z}_{t+1}, \hat{s}_{t+1}, x_t) \right) \right] \\ &= \mathbb{E}_t \left[\exp \left(-\bar{r} - (e_3 - e_2B)A^{-1}\tilde{Z}_t - \frac{\gamma}{2}(1 - \theta_0)(1 - 2\hat{s}_t) \right. \right. \\ &\quad \left. \left. - \gamma(1 + \lambda(\hat{s}_t))\sigma_c \epsilon_{1,t+1} + b_{n-1}(\tilde{Z}_{t+1}, \hat{s}_{t+1}, x_t) \right) \right]. \end{aligned} \quad (\text{A136})$$

The recursion for nominal bond prices with $n \geq 3$ is similar. It is complicated by the fact that we need to integrate over long-term monetary policy shocks, which are not necessarily spanned by ϵ_{t+1} :

$$B_n^{\$}(\tilde{Z}_t, \hat{s}_t, x_{t-1}) = \mathbb{E}_t \left[\exp \left(m_{t+1} - Y_{2,t+1} - n v_{t+1}^{LT} + b_{n-1}^{\$}(\tilde{Z}_{t+1}, \hat{s}_{t+1}, x_t) \right) \right]. \quad (\text{A137})$$

To reduce the number of dimensions along which we need to integrate numerically, we split v_{t+1}^{LT} into a component that is spanned by ϵ_{t+1} plus an orthogonal shock. This is useful because we can then use analytic expressions to integrate over the orthogonal component. We use the standard expression for conditional distributions of multivariate normal random variables. The distribution of v_{t+1}^{LT} conditional on ϵ_{t+1} is normal with:

$$v_{t+1}^{LT} | \epsilon_{t+1} \sim N \left(\underbrace{(A \Sigma \Sigma_v e'_4)' \epsilon_{t+1}}_{vec^*}, \underbrace{(\sigma_{LT})^2 - (A \Sigma \Sigma_v e'_4)' (A \Sigma \Sigma_v e'_4)}_{\sigma_{\perp}^2} \right). \quad (\text{A138})$$

We then write v_t^{LT} as the sum of two independent shocks:

$$v_{t+1}^{LT} = vec^* \epsilon_{t+1} + \epsilon_{t+1}^{\perp}, \quad (\text{A139})$$

where ϵ_{t+1}^{\perp} is defined as

$$\epsilon_{t+1}^{\perp} := v_{t+1}^{LT} - vec^* \epsilon_{t+1} \quad (\text{A140})$$

We integrate analytically over ϵ_{t+1}^{\perp} in equation (A141):

$$\begin{aligned} B_n^{\$}(\tilde{Z}_t, \hat{s}_t, x_{t-1}) &= \mathbb{E}_t \left[\exp \left(m_{t+1} - Y_{2,t+1} - n vec^* \epsilon_{t+1} + \frac{n^2}{2} (\sigma_{\perp})^2 + b_{n-1}^{\$}(\tilde{Z}_{t+1}, \hat{s}_{t+1}, B^{\$} x_t) \right) \right], \\ &= \mathbb{E}_t \left[\exp \left(-\bar{r} - e_3 A^{-1} \tilde{Z}_t - \frac{\gamma}{2} (1 - \theta_0) (1 - 2\hat{s}_t) \right. \right. \\ &\quad \left. \left. - (\gamma(1 + \lambda(\hat{s}_t))\sigma_c + \underbrace{e_2 A^{-1} e'_1 + n vec^* e'_1}_{vpi_1}) \epsilon_{1,t+1} \right. \right. \\ &\quad \left. \left. - \left(\underbrace{e_2 A^{-1} e'_2 + n vec^* e'_2}_{vpi_2} \right) \epsilon_{2,t+1} \right. \right. \\ &\quad \left. \left. + \frac{n^2}{2} (\sigma_{\perp})^2 + b_{n-1}^{\$}(\tilde{Z}_{t+1}, \hat{s}_{t+1}, x_t) \right) \right]. \quad (\text{A141}) \end{aligned}$$

We define the vectors vpi_1 and vpi_2 as given above to avoid computing them repeatedly in our numerical algorithm.

C.5.3 Computing returns

The log return on the consumption claim equals:

$$r_{t+1}^c = \log\left(\frac{P_{t+1}^c + C_{t+1}}{P_t^c}\right), \quad (\text{A142})$$

$$= \Delta c_{t+1} + \log\left(\frac{1 + \frac{P_{t+1}^c}{C_{t+1}}}{\frac{P_t^c}{C_t}}\right). \quad (\text{A143})$$

Real and nominal log bond yields equal:

$$y_{n,t} = -\frac{1}{n}b_{n,t}, \quad (\text{A144})$$

$$y_{n,t}^{\$} = -\frac{1}{n}b_{n,t}^{\$} + \pi_t^*. \quad (\text{A145})$$

Real log bond returns equal:

$$r_{n,t+1} = b_{n-1,t+1} - b_{n,t}. \quad (\text{A146})$$

Nominal log bond returns equal:

$$r_{n,t+1}^{\$} = b_{n-1,t+1}^{\$} - b_{n,t}^{\$} - (n-1)v_{t+1}^* + nv_t^*. \quad (\text{A147})$$

Real and nominal bond log excess returns then equal:

$$xr_{n,t+1} = r_{n,t+1} - r_t, \quad (\text{A148})$$

$$xr_{n,t+1}^{\$} = r_{n,t+1}^{\$} - i_t. \quad (\text{A149})$$

C.5.4 Levered stock prices and returns

We note that the price of the levered equity claim is δP_t^c , so the price-dividend ratio equals:

$$\frac{P_t^\delta}{D_t^\delta} = \delta \frac{C_t}{D_t^\delta} \frac{P_t^c}{C_t}. \quad (\text{A150})$$

Using the expression

$$D_{t+1}^\delta = P_{t+1}^c + C_{t+1} - (1-\delta)P_t^c \exp(r_t) - \delta P_t^c, \quad (\text{A151})$$

and

$$P_t^\delta = \delta P_t^c \quad (\text{A152})$$

gives the gross return on levered stocks:

$$(1 + R_{t+1}^\delta) = \frac{D_{t+1}^\delta + P_{t+1}^\delta}{P_t^\delta}, \quad (\text{A153})$$

$$= \frac{1}{\delta} \frac{P_{t+1}^c + C_{t+1} - (1 - \delta)P_t^c \exp(r_t)}{P_t^c}, \quad (\text{A154})$$

$$= \frac{1}{\delta} (1 + R_{t+1}^c) - \frac{1 - \delta}{\delta} \exp(r_t). \quad (\text{A155})$$

Log stock excess returns then equal:

$$xr_{t+1}^\delta = r_{t+1}^\delta - r_t. \quad (\text{A156})$$

To mimic firms' dividend smoothing in the data, we report simulated moments for the price of equities dividend by dividends smoothed over the past 64 quarters:

$$P_t^\delta / \left(\frac{1}{64} (D_t^\delta + D_{t-1}^\delta + \dots + D_{t-63}^\delta) \right). \quad (\text{A157})$$

C.6 Risk-premium decomposition

We use the superscript rn for risk-neutral, superscript cf for cash flow, and rp for risk premium. Risk-neutral valuations are expected cash flows discounted with the risk-neutral discount factor, that is consistent with equilibrium dynamics for the real interest rate:

$$M_{t+1}^{rn} = \exp(-r_t). \quad (\text{A158})$$

C.6.1 Risk-neutral zero-coupon bond prices

We use analogous recursions to solve for risk-neutral bond prices. One-period risk-neutral bond prices are given exactly as before by equations (A128) and (A129). For $n > 1$, we guess and verify that the prices of real and nominal risk-neutral zero-coupon bonds with maturity n can be written in the following form

$$P_{n,t}^{rn} = B_n^{rn}(\tilde{Z}_t, \hat{s}_t, x_{t-1}), \quad (\text{A159})$$

$$P_{n,t}^{\$,rn} = \exp(-nv_t^*) B_n^{\$,rn}(\tilde{Z}_t, \hat{s}_t, x_{t-1}). \quad (\text{A160})$$

for some functions $B_n^{rn}(\tilde{Z}_t, \hat{s}_t, x_{t-1})$ and $B_n^{\$,rn}(\tilde{Z}_t, \hat{s}_t, x_{t-1})$.

We derive the two-period risk-neutral nominal bond price analytically:

$$P_{2,t}^{\$,rn} = \exp(-r_t) \mathbb{E}_t \left[P_{1,t+1}^{\$,rn} \exp(-v_{t+1}^* - Y_{2,t+1}) \right] \quad (\text{A161})$$

$$= \exp(-r_t) \mathbb{E}_t \left[\exp(-Y_{3,t+1} - 2v_{t+1}^* - Y_{2,t+1} - \bar{r}) \right]. \quad (\text{A162})$$

We can hence verify that the two-period risk-neutral nominal bond price takes the form (A127)

$$b_2^{\$,rn} = -e_3 [I + B] A^{-1} \tilde{Z}_t + \frac{1}{2} v_{\$} \Sigma_u v_{\$}' - 2\bar{r} \quad (\text{A163})$$

Here, the vector v_{\S} is identical to the case with risk aversion. Comparing expressions (A163) and (A133) shows that they agree when $\gamma = 0$. We similarly solve for 2-period real bond prices in closed form:

$$P_{2,t}^{rn} = \exp(-Y_{3,t} + \mathbb{E}_t Y_{2,t+1} - \bar{r}) \times \exp(\mathbb{E}_t(-Y_{3,t+1} + \mathbb{E}_{t+1} Y_{2,t+2} - \bar{r})) \\ \times \mathbb{E}_t \left[\exp \left(- \underbrace{(e_3 - e_2 B) \Sigma v_{t+1}}_{v_r} \right) \right]. \quad (\text{A164})$$

The vector v_r is again identical to the case with risk aversion. Taking logs gives:

$$b_2^{rn}(\tilde{Z}_t, \hat{s}_t, x_{t-1}) = -(e_3 - e_2 B) [I + B] A^{-1} \tilde{Z}_t + \frac{1}{2} v_r \Sigma_u v_r' - 2\bar{r}. \quad (\text{A165})$$

We note that the risk-neutral bond prices (A165) and bond prices with risk aversion (A135) are identical when the utility curvature parameter γ equals zero.

For $n \geq 3$ the n -period risk neutral real bond price B_n^{rn} satisfies the recursion:

$$B_n^{rn}(\tilde{Z}_t, \hat{s}_t, x_{t-1}) = \mathbb{E}_t \left[\exp \left(-\bar{r} - (e_3 - e_2 B) A^{-1} \tilde{Z}_t + b_{n-1}(\tilde{Z}_{t+1}, \hat{s}_{t+1}, x_t) \right) \right] \quad (\text{A166})$$

We obtain a similar recursion for risk-neutral nominal bond prices:

$$B_n^{\$,rn}(\tilde{Z}_t, \hat{s}_t, x_{t-1}) = \mathbb{E}_t \left[\exp \left(Y_{3,t} + \mathbb{E}_t Y_{2,t+1} - \bar{r} - Y_{2,t+1} - n v_{t+1}^* + b_{n-1}^{\$}(\tilde{Z}_{t+1}, \hat{s}_{t+1}, x_t) \right) \right].$$

We again use the decomposition $v_{t+1}^* = vec^* \epsilon_{t+1} + \epsilon_{t+1}^{\perp}$ from Section C.5.2 to reduce the dimensionality of the numerical integration:

$$B_n^{\$,rn}(\tilde{Z}_t, \hat{s}_t, x_{t-1}) = \mathbb{E}_t \left[\exp \left(-Y_{3,t} + \mathbb{E}_t Y_{2,t+1} - \bar{r} - Y_{2,t+1} - n \cdot vec^* \epsilon_{t+1} + \frac{n^2}{2} (\sigma^{\perp})^2 \right. \right. \\ \left. \left. + b_{n-1}^{\$}(\tilde{Z}_{t+1}, \hat{s}_{t+1}, x_t) \right) \right], \quad (\text{A167}) \\ = \mathbb{E}_t \left[\exp \left(-\bar{r} - e_3 A^{-1} \tilde{Z}_t - \underbrace{(e_2 A^{-1} e_1' + n \cdot vec^* e_1')}_{v_{pi_1}} \epsilon_{1,t+1} \right. \right. \\ \left. \left. - \left(\underbrace{e_2 A^{-1} e_2'}_{v_{pi_2}} + n \cdot vec^* e_2' \right) \epsilon_{2,t+1} + \frac{n^2}{2} (\sigma^{\perp})^2 + b_{n-1}^{\$}(\tilde{Z}_{t+1}, \hat{s}_{t+1}, x_t) \right) \right]. \quad (\text{A168})$$

C.6.2 Risk-neutral zero-coupon consumption claims

Next, we derive recursive solutions for the risk-neutral prices of zero-coupon consumption claims. Let $P_{nt}^{c,rn}/C_t$ denote the risk-neutral price-dividend ratio of a zero-coupon claim on consumption at time $t+n$. The risk-neutral price-consumption ratio of a claim to the

entire stream of future consumption equals:

$$\frac{P_t^{c, rn}}{C_t} = \sum_{n=1}^{\infty} \frac{P_{nt}^{c, rn}}{C_t}. \quad (\text{A169})$$

For $n \geq 1$, we guess and verify there exists a function $F_n^{rn}(\tilde{Z}_t, \hat{s}_t, x_{t-1})$, such that

$$\frac{P_{nt}^{c, rn}}{C_t} = F_n^{rn}(\tilde{Z}_t, \hat{s}_t, x_{t-1}). \quad (\text{A170})$$

We start by deriving the analytic expression for F_1^{rn} . The one-period risk-neutral zero-coupon price-consumption ratio solves

$$\frac{P_{1,t}^{c, rn}}{C_t} = \exp(-Y_{3,t} + \mathbb{E}_t Y_{2,t+1} - \bar{r}) \mathbb{E}_t \left[\frac{C_{t+1}}{C_t} \right] \quad (\text{A171})$$

Using (21) to substitute for consumption growth, we can derive the following analytic expression for f_1^{rn} :

$$f_1^{rn}(\tilde{Z}_t, \hat{s}_t, x_{t-1}) = -(1 - \rho^a)(e_3 - e_2 B) A^{-1} \tilde{Z}_t - \bar{r} + g + e_1 [B - \phi I] A^{-1} \tilde{Z}_t + \frac{1}{2} \sigma_c^2. \quad (\text{A172})$$

Next, we solve for f_n , $n \geq 2$ iteratively:

$$\frac{P_{nt}^{c, rn}}{C_t} = \exp(-Y_{3,t} + \mathbb{E}_t Y_{2,t+1} - \bar{r}) \mathbb{E}_t \left[\frac{C_{t+1}}{C_t} F_{n-1}^{rn}(\tilde{Z}_{t+1}, \hat{s}_{t+1}, x_t) \right] \quad (\text{A173})$$

This gives the following expression for f_n^{rn} :

$$f_n^{rn}(\tilde{Z}_t, \hat{s}_t, x_{t-1}) = \log \left[\mathbb{E}_t \left[\exp \left(-(1 - \rho^a)(Y_{3,t} + \mathbb{E}_t Y_{2,t+1}) - \bar{r} + g - \phi x_t + \mathbb{E}_t x_{t+1} + \sigma_c \epsilon_{1,t+1} + f_{n-1}^{rn}(\tilde{Z}_{t+1}, \hat{s}_{t+1}, x_t) \right) \right] \right]. \quad (\text{A174})$$

Finally, we re-write $f_{n,t}^{rn}$ as an expectation involving $f_{n-1,t+1}^{rn}$, the state variables \tilde{Z}_t , and period $t + 1$ shocks:

$$f_n^{rn}(\tilde{Z}_t, \hat{s}_t, x_{t-1}) = \log \left[\mathbb{E}_t \left[\exp \left(g + e_1 [B - \phi I] A^{-1} \tilde{Z}_t - \bar{r} - (1 - \rho^a)(e_3 - e_2 B) A^{-1} \tilde{Z}_t + \sigma_c \epsilon_{1,t+1} + f_{n-1}^{rn}(\tilde{Z}_{t+1}, \hat{s}_{t+1}, x_t) \right) \right] \right]. \quad (\text{A175})$$

C.6.3 Risk-neutral returns

We plug risk-neutral price-consumption ratios and bond prices into equations (A143) through (A149). This gives risk-neutral returns on the consumption claim, risk-neutral log excess bond returns, and risk-neutral bond yields. We then substitute risk-neutral returns on the consumption claim into (A155)-(A156) to obtain risk-neutral log excess stock returns.

C.7 Modeling FOMC High-Frequency Asset Prices

In order to simulate high-frequency changes in stocks and bonds around FOMC announcements, we decompose the quarterly shock into a pre-FOMC and an FOMC component, which are assumed to be uncorrelated

$$v_t = v_t^{pre} + v_t^{FOMC}. \quad (\text{A176})$$

We therefore effectively model FOMC dates as occurring always at the end of the quarter, because that is the only date when we compute asset prices. The variance-covariance matrix of shocks released prior to the FOMC announcement is

$$\Sigma_v^{pre} = \Sigma_v - \text{diag}([\sigma_x^{FOMC}, \sigma_\pi^{FOMC}, \sigma_{ST}^{FOMC}, \sigma_{LT}^{FOMC}]). \quad (\text{A177})$$

We then split the rotated ϵ_t shock similarly according to

$$\epsilon_t^{pre} = A\Sigma v_t^{pre}, \quad (\text{A178})$$

$$\epsilon_t^{FOMC} = A\Sigma v_t^{FOMC}. \quad (\text{A179})$$

The aggregate dynamics and asset pricing solution are of course unchanged to before, because the distribution of quarterly fundamental shocks v_t is unchanged. But splitting it into two independent shocks allows us to differentiate asset prices before vs. after the FOMC shock v_t^{FOMC} .

We compute pre-FOMC asset prices very simply at the expected quarter t state vector before the FOMC shock is realized. The expected pre-FOMC state variables plus consumption are given by

$$\tilde{Z}_t^{pre} = \tilde{P}\tilde{Z}_{t-1} + \epsilon_t^{pre}, \quad (\text{A180})$$

$$Y_t^{pre} = PY_{t-1} + A^{-1}\epsilon_t^{pre}, \quad (\text{A181})$$

$$\hat{s}_t^{pre} = \theta_0\hat{s}_{t-1} + \theta_1Y_{1,t-1} + \theta_2Y_{1,t-2} + \dots\lambda(\hat{s}_{t-1}, \bar{S})\sigma_c\epsilon_{1,t}^{pre}, \quad (\text{A182})$$

$$c_t^{pre} = g + c_{t-1} + (Y_{1,t}^{pre} - \phi Y_{1,t-1}), \quad (\text{A183})$$

$$v_t^{*,pre} = v_{t-1}^* + v_t^{LT,pre}. \quad (\text{A184})$$

We compute pre-FOMC stock and bond prices by substituting the pre-FOMC state vector into the solutions from the asset pricing value function iterations:

$$\frac{P_t^{pre}}{C_t^{pre}} = F(\tilde{Z}_t^{pre}, \hat{s}_t^{pre}, x_{t-1}), \quad (\text{A185})$$

$$P_{n,t}^{\$,pre} = \exp(-nv_t^{*,pre}) B_n^{\$}(\tilde{Z}_t^{pre}, \hat{s}_t^{pre}, x_{t-1}), \quad (\text{A186})$$

$$P_{n,t}^{pre} = B_n(\tilde{Z}_t^{pre}, \hat{s}_t^{pre}, x_{t-1}) \quad (\text{A187})$$

The pre-FOMC nominal and real log bond yields are then given by

$$y_{n,t}^{\$,pre} = -n \log(P_{n,t}^{\$,pre}), \quad (\text{A188})$$

$$y_{n,t}^{pre} = -n \log(P_{n,t}^{pre}). \quad (\text{A189})$$

Pre-FOMC breakeven is computed as

$$breakeven_{n,t}^{pre} = y_{n,t}^{\$,pre} - y_{n,t}^{pre}. \quad (\text{A190})$$

We then compute simulated changes in the short-term nominal interest rate, as well as long-term bond yields and breakeven around FOMC announcements

$$\Delta i_t^{FOMC} = (Y_{3,t} + v_t^*) - (Y_{3,t}^{pre} + v_t^{*,pre}), \quad (\text{A191})$$

$$\Delta y_{n,t}^{\$,FOMC} = y_{n,t}^{\$} - y_{n,t}^{\$,pre}, \quad (\text{A192})$$

$$\Delta y_{n,t}^{FOMC} = y_{n,t} - y_{n,t}^{pre}, \quad (\text{A193})$$

$$\Delta breakeven_{n,t}^{FOMC} = breakeven_{n,t} - breakeven_{n,t}^{pre}. \quad (\text{A194})$$

Stock returns around the FOMC date are computed assuming that no consumption takes place during the FOMC interval (equivalently, the FOMC interval is infinitesimal), so

$$r_t^{c,FOMC} = \log \left(\exp(c_t - c_t^{pre}) \frac{\frac{P_t^c}{C_t}}{\frac{P_t^{c,pre}}{C_t^{pre}}} \right). \quad (\text{A195})$$

The levered return around the FOMC date then is

$$r_t^{\delta,FOMC} = \log((1/\delta)\exp(r_t^{c,FOMC}) - ((1 - \delta)/\delta)), \quad (\text{A196})$$

which follows from using the standard formula for levered stock returns while setting the real interest rate and consumption to zero, because the FOMC interval is infinitesimal.

D Solving for Asset Prices numerically

We evaluate asset prices by iterating on a grid for the state vector as in [Campbell, Pflueger, and Viceira \(2020\)](#) building on [Wachter \(2005\)](#). Other numerical methodologies are faster, but their cost is that they cannot replicate the economic properties of [Wachter \(2005\)](#)'s numerical solution for Campbell-Cochrane. [Lopez, López-Salido, and Vazquez-Grande \(2018\)](#) develop an analytically convenient solution method, that approximates the sensitivity function λ by an affine function. While their method is analytically more convenient than ours, their Figure 1 shows an average price-dividend ratio of around 25 for the original Campbell and Cochrane (1999) model, whereas Wachter (2005)'s numerical best practices yield a price-dividend ratio of 35. Figure 1 in [Lopez, López-Salido, and Vazquez-Grande \(2018\)](#) also shows clearly that perturbation methods and global solution methods generate similarly economically meaningful differences with Wachter (2005)'s best practice numerical solution. In unreported results, we verified that analytic affine approximations to the sensitivity function λ (such as in [Lopez, López-Salido, and Vazquez-Grande 2015](#)), numerical higher-order perturbation methods using Dynare ([Rudebusch and Swanson 2008](#)), and global projection methods give solutions for Campbell-Cochrane that are economically very different from Wachter (2005)'s numerical solution. We therefore follow the practice of Wachter (2005) and extend the

numerical grid solution to our setting with multiple state variables, which is facilitated by the log-linear dynamics of macroeconomic state variables.

Other approaches in the literature are also not appropriate for our problem. While Chen (2017) solves a model with habit and production using global projection and perturbation methods, his model features a linear sensitivity function and heteroskedastic consumption. Andreasen (2020) also uses perturbation methods for a model with heteroskedastic shocks. By contrast, we have homoskedastic consumption and the highly nonlinear sensitivity function required to make the real risk-free rate well-behaved means that perturbation methods do not work well. Similarly, affine term structure models, such as Dai and Singleton (2000), generate affine relations between risk premia and state variables by assuming analytically convenient functional forms for the pricing kernel. In contrast to models that assume more convenient pricing kernels, our preferences are consistent with the standard log-linear New Keynesian consumption Euler equation and generate conditionally homoskedastic macroeconomic dynamics.

While iterating on a grid is significantly slower than perturbation or global projection methods, it is not prohibitively so. Our MATLAB algorithm for solving the asset pricing recursions (described in Section D.1) takes 94 seconds to run on a Lenovo X280 laptop with an i7-8650U CPU. Simulating the model (described in Section D.2) takes 35 seconds. The risk-neutral asset pricing recursions and simulating the risk-neutral stock returns take an additional 88 seconds and 37 seconds.

D.1 Implementing the asset pricing recursions

We implement the recursions in Sections C.5.1 and C.5.2 numerically through value function iteration on a grid. We solve for the functions f_n , b_n , and b_n^s using value function iteration along a five-dimensional state vector. We use a five-dimensional grid, with the first three dimensions corresponding to \tilde{Z}_t , the fourth dimension corresponding to \hat{s}_t , and the fifth dimension corresponding to x_{t-1} .

D.1.1 Grid

In this section, we use \tilde{Z}, \hat{s}, x to denote the corresponding time- t variables. We use superscripts $-$ to denote variables in the previous period and $+$ to denote variables in the next period. We solve numerically for f_n , b_n , and b_n^s as functions of the vector of state variables $[\tilde{Z}, \hat{s}, x^-]$.

Our grid is densest along the \hat{s} dimension to capture important non-linearities of asset prices with respect to the surplus consumption ratio. Following Wachter (2005), we choose a grid for the surplus consumption ratio that consists of an upper segment and a lower segment and covers a wide range of values for s_t . Let $S_{grid,1}$ denote a vector of 20 equally spaced points between 0 and S_{max} with S_{max} included and $s_{grid,2}$ a vector of 30 equally spaced points between $\min(\log(S_{grid,1}))$, and -50 . The grid for $\hat{s}_t = s_t - \bar{s}$ then consists of the concatenation of $s_{grid,2} - \bar{s}$ and $\log(S_{grid,1}) - \bar{s}$.

We find that bond and stock prices are close to loglinear in \tilde{Z} and \hat{x}^- , so coarser grids are sufficient along those dimensions of the state vector. In fact, the analytic expressions for f_1 , b_2 , and b_2^s show that one-period zero-coupon consumption claims and two-period bond prices are exactly log-linear in \tilde{Z} and x^- . Numerical results indicate that this

property translates to longer-period claims and f_n , b_n , and b_n^s are still approximately linear in \tilde{Z} and x^- for general n . To speed up the value function iteration, we therefore use two grid points for each dimension of \tilde{Z} and for x^- .

For \tilde{Z} , we use an equal-spaced three-dimensional grid. Let N denote the number of grid points along each dimension and m the width of the grid as a multiple of the unconditional standard deviation of \tilde{Z} . For each dimension of \tilde{Z} , we choose a grid of N equal-spaced points with the lowest point equal to $-m \times std(\tilde{Z})$ and the highest point equal to $m \times std(\tilde{Z})$. Here, the unconditional variance-covariance matrix of \tilde{Z} is determined implicitly by the equation:

$$std(\tilde{Z}) = \sqrt{\tilde{B}Var(\tilde{Z})\tilde{B}' + diag(1, 1, 1)}. \quad (\text{A197})$$

For our baseline grid, we set $N = 2$ and $m = 2$.

For x^- , we consider an equal-spaced grid with $sizexm$ points ranging from $\min(e_1 A \tilde{Z}_t : \tilde{Z} \in grid)$ to $\max(e_1 A \tilde{Z} : \tilde{Z} \in grid)$. This choice of grid ensures that the grid for x^- covers the entire range of output gap values implied by the grid for \tilde{Z} . In our baseline evaluation, we set $sizexm = 2$.

With $N = 2$ grid points along each of the three dimensions of \tilde{Z} , 50 gridpoints for \hat{s} , and $sizexm = 2$ grid points for x^- , the combined grid has a total of $2^3 \cdot 50 \cdot 2 = 800$ points.

D.1.2 Numerical integration

Following Wachter (2005), we use Gauss-Legendre quadrature to evaluate the expectations (A125), (A136), and (A141) numerically. Gauss-Legendre quadrature is orders of magnitude faster than computing expectations by simulation. As in Wachter (2005), we evaluate infinite integrals over the density of standardized consumption shocks ($\epsilon_{1,t}$) using 40 integration node points and an integration domain ranging from -8 standard deviations to $+8$ standard deviations. To conserve speed and memory, we integrate over shocks orthogonal to surplus consumption ($\epsilon_{2,t}$) using a somewhat smaller number of integration node points, 15, but again an integration domain of ± 8 standard deviations. To evaluate bond and stock prices at points that are not on the grid, we use loglinear multi-linear interpolation and extrapolation.

For completeness, we recap the key features of Gauss-Legendre integration. Let xGL_i , $i = 1, \dots, N_{GL}$ and $wGL_i = 1, \dots, N_{GL}$ denote the Gauss-Legendre nodes and weights of N_{GL} th order. Gauss-Legendre quadrature then approximates a definite integral of any smooth function f on the interval $[-1, 1]$ by $\int_{-1}^1 f(x) dx \approx \sum_{i=1}^{N_{GL}} wGL_i f(xGL_i)$. By change of variable, it is immediate that we can approximate the integral of a smooth function f on an interval $[-\bar{a}, \bar{a}]$ by

$$\int_{-\bar{a}}^{\bar{a}} f(x) dx \approx \sum_{i=1}^{N_{GL}} \underbrace{\bar{a} \times wGL_i}_{wGL_i^{\bar{a}}} f\left(\underbrace{\bar{a} \times xGL_i}_{xGL_i^{\bar{a}}}\right). \quad (\text{A198})$$

Here, we use $xGL_i^{\bar{a}}$ and $wGL_i^{\bar{a}}$ to denote Gauss-Legendre node points and weights scaled to the interval $[-\bar{a}, \bar{a}]$.

We implement Gauss-Legendre quadrature to take expectations over ϵ_{t+1} as follows. Let N_1 denote the number of Gauss-Legendre nodes and \bar{a}_1 denote the integration domain for the shock $\epsilon_{1,t}$, that is perfectly correlated with output innovations. We set $xGL_{1,i} = xGL_i^{\bar{a}_1}$ and $wGL_{1,i} = wGL_i^{\bar{a}_1}$ for $i = 1, \dots, N_1$, where the weights and nodes are as defined in equation (A198). Moreover, we set

$$pGL_{1,i} = \frac{1}{\sqrt{2\pi}} \exp(-xGL_{1,i}^2) wGL_{1,i} / \sum_{i=1}^{N_1} \left(\frac{1}{\sqrt{2\pi}} \exp(-xGL_{1,i}^2) wGL_{1,i} \right), \quad (\text{A199})$$

and use the scaled weights $pGL_{1,i}$ for numerical integration. The scaling of (A199) ensures that the numerical expectation of a constant is evaluated to be the same constant (or intuitively that discretized probabilities sum to one).

We then evaluate numerically the expectation of any smooth function f of $\epsilon_{1,t}$ via:

$$E[f(\epsilon_{1,t})] = \int_{-\infty}^{\infty} \frac{1}{\sqrt{2\pi}} \exp(-\epsilon_1^2) f(\epsilon_1) d\epsilon_1, \quad (\text{A200})$$

$$\approx \int_{-\bar{a}_1}^{\bar{a}_1} \frac{1}{\sqrt{2\pi}} \exp(-\epsilon_1^2) f(\epsilon_1) d\epsilon_1, \quad (\text{A201})$$

$$\approx \sum_{i=1}^{N_1} pGL_{1,i} f(xGL_{1,i}). \quad (\text{A202})$$

Accuracy increases with \bar{a}_1 and N_1 . We follow Wachter (2006) in setting $N_1 = 40$ and $\bar{a}_1 = 8$.

To take expectations over $\epsilon_{2,t}$ and $\epsilon_{3,t}$, we similarly use Gauss-Legendre quadrature with integration domain $\bar{a}_2 = 8$ and number of nodes $N_2 = 15$. We set $xGL_{2,i} = xGL_i^{\bar{a}_2}$ and $wGL_{2,i} = wGL_i^{\bar{a}_2}$ for $i = 1, \dots, N_2$ and define the scaled weights:

$$pGL_{2,i} = \frac{1}{\sqrt{2\pi}} \exp(-xGL_{2,i}^2) wGL_{2,i} / \sum_{i=1}^{N_2} \left(\frac{1}{\sqrt{2\pi}} \exp(-xGL_{2,i}^2) wGL_{2,i} \right), \quad (\text{A203})$$

The weights and nodes for $\epsilon_{3,t}$ are identical to those of $\epsilon_{2,t}$.

Since $\epsilon_{1,t}$, $\epsilon_{2,t}$, and $\epsilon_{3,t}$ are independent, we can evaluate the expectation of any smooth function $f(\epsilon_{1,t}, \epsilon_{2,t}, \epsilon_{3,t})$ as

$$\begin{aligned} Ef(\epsilon_{1,t}, \epsilon_{2,t}, \epsilon_{3,t}) &= \int_{-\infty}^{\infty} \frac{1}{\sqrt{2\pi}} \exp(-\epsilon_1^2) \int_{-\infty}^{\infty} \frac{1}{\sqrt{2\pi}} \exp(-\epsilon_2^2) \int_{-\infty}^{\infty} \frac{1}{\sqrt{2\pi}} \exp(-\epsilon_3^2) f(\epsilon_1, \epsilon_2, \epsilon_3) d\epsilon_1 d\epsilon_2 d\epsilon_3 \\ &\approx \sum_{i=1}^{N_1} pGL_{1,i} \left[\sum_{j=1}^{N_2} pGL_{2,j} \left[\sum_{k=1}^{N_3} pGL_{3,k} f(xGL_{1,i}, xGL_{2,j}, xGL_{3,k}) \right] \right]. \end{aligned} \quad (\text{A204})$$

D.1.3 Recursive step

Let a superscript num denote the numerical counterparts to the analytic functions f_n , b_n , b_n^s . We start by initializing $f_1^{num}(\tilde{Z}, \hat{s}, x^-)$, $b_2^{num}(\tilde{Z}, \hat{s}, x^-)$, and $b_2^{s,num}(\tilde{Z}, \hat{s}, x^-)$ at each grid point according to the analytic expressions (A123), (A133) and (A135).

Next, we apply the recursive expressions (A125), (A136), and (A141) along the grid.

Having computed f_{n-1}^{num} along the entire grid, we evaluate $f_n^{num}(\tilde{Z}, \hat{s}, x^-)$ at a grid point $(\tilde{Z}, \hat{s}, x^-)$ as follows. We compute the expectation (A125) numerically as:

$$\begin{aligned}
f_n^{num}(\tilde{Z}, \hat{s}, x^-) = & \log \left[\sum_{i=1}^{N_1} pGL_{1,i} \left[\sum_{j=1}^{N_2} pGL_{2,j} \left[\sum_{k=1}^{N_3} pGL_{3,k} \cdot \exp \left(g + e_1[B - \phi I]A^{-1}\tilde{Z} \right. \right. \right. \right. \\
& - \bar{r} - (1 - \rho^a)(e_3 - e_2B)A^{-1}\tilde{Z} - \frac{\gamma}{2}(1 - \theta_0)(1 - 2\hat{s}) \\
& \left. \left. \left. - (\gamma(1 + \lambda(\hat{s})) - 1)\sigma_c \times xGL_{1,i} \right. \right. \right. \\
& \left. \left. \left. + f_{n-1}^{num} \left(\tilde{B}\tilde{Z} + \begin{bmatrix} xGL_{1,i} \\ xGL_{2,j} \\ xGL_{3,k} \end{bmatrix}, \theta_0\hat{s} + \theta_1x + \theta_2x^- + \lambda(\hat{s})xGL_{1,i}, x \right) \right] \right] \right], \tag{A205}
\end{aligned}$$

where we evaluate x as a function of the state vector as

$$x = e_1A^{-1}\tilde{Z}. \tag{A206}$$

To compute the right-hand-side of (A205), we need to evaluate f_{n-1}^{num} at points that are not on our grid. We interpolate f_{n-1}^{num} linearly (and hence F_{n-1}^{num} log-linearly). When the argument is outside the range of the grid, we extrapolate f_{n-1}^{num} linearly. It is clear from (A123) that linear inter- and extrapolation gives a good approximation of f_1 . In fact, we can see that f_1 is exactly linear in \tilde{Z} , independent of x^- , and that it depends on $\lambda(\hat{s}) = \lambda_0\sqrt{1 - 2\hat{s}}$. We accommodate the fact that f_1 is not linear in \hat{s} by choosing a much denser grid along the \hat{s} dimension. We do not have analytic expressions for $f_n, n > 1$ (after all, that's why we need a numerical solution), but numerical solutions indicate that linear inter- and extrapolation gives good approximations for f_n with the chosen grid.

In terms of coding (A205), we face a trade-off between speed and readability of the code. We pre-allocate matrices outside loops and we code linear interpolation by hand (rather than using a pre-written interpolation routine) to conserve speed and memory. We also inline the linear interpolation steps (i.e. write them directly into the main function rather than calling a separate interpolation function). This speeds up the code substantially, while reducing its readability.

There are different methods to interpolate multidimensional functions. Specifically, we use multi-linear interpolation, corresponding to interpolating along each dimension one at a time. In order to enhance computational speed we do not rely on a pre-programmed interpolation routine, instead coding our own minimal interpolation routine. It is well-known that the result of multi-linear (or in the two-dimensional case bi-linear) interpolation does not depend on in which order one interpolates the different arguments. We find it convenient to interpolate $f_{n-1}^{num}(\tilde{Z}, \hat{s}, x^-)$ first along the x^- dimension, then along \hat{s} , then along \tilde{Z}_1 , and finally along the \tilde{Z}_2 and \tilde{Z}_3 dimensions.

Finally, we evaluate the price-consumption ratio for the aggregate consumption stream by approximating it as the sum of the first 300 zero-coupon consumption claims:

$$F^{num}(\tilde{Z}_t, \hat{s}_t, x_{t-1}) = \sum_{n=1}^{300} \exp \left(f_n^{num}(\tilde{Z}_t, \hat{s}_t, x_{t-1}) \right). \tag{A207}$$

We iterate $b_n^{num}(\tilde{Z}, \hat{s}, x^-)$ and $b_n^{\$,num}(\tilde{Z}, \hat{s}, x^-)$ similarly according to:

$$\begin{aligned}
b_n^{num}(\tilde{Z}_t, \hat{s}_t, x_{t-1}) &= \log \left[\sum_{i=1}^{N_1} pGL_{1,i} \left[\sum_{j=1}^{N_2} pGL_{2,j} \left[\sum_{k=1}^{N_3} pGL_{3,k} \right. \right. \right. \\
&\quad \cdot \exp \left(-\bar{r} - (e_3 - e_2 B) A^{-1} \tilde{Z} - \frac{\gamma}{2} (1 - \theta_0) (1 - 2\hat{s}) \right. \\
&\quad \left. \left. \left. - \gamma (1 + \lambda(\hat{s})) \sigma_c \times xGL_{1,i} \right. \right. \right. \\
&\quad \left. \left. \left. + b_{n-1}^{num} \left(\tilde{B} \tilde{Z} + \begin{bmatrix} xGL_{1,i} \\ xGL_{2,j} \\ xGL_{3,k} \end{bmatrix}, \theta_0 \hat{s} + \theta_1 x + \theta_2 x^- + \lambda(\hat{s}) xGL_{1,i}, x \right) \right] \right] \right], \tag{A208}
\end{aligned}$$

and

$$\begin{aligned}
b_n^{\$,num}(\tilde{Z}_t, \hat{s}_t, x_{t-1}) &= \left[\sum_{i=1}^{N_1} pGL_{1,i} \left[\sum_{j=1}^{N_2} pGL_{2,j} \left[\sum_{k=1}^{N_3} pGL_{3,k} \right. \right. \right. \tag{A209} \\
&\quad \cdot \exp \left(-\bar{r} - e_3 A^{-1} \tilde{Z} - \frac{\gamma}{2} (1 - \theta_0) (1 - 2\hat{s}) \right. \\
&\quad \left. - (\gamma (1 + \lambda(\hat{s})) \sigma_c + vpi_1 + n \cdot vec^* e'_1) \times xGL_{1,i} \right. \\
&\quad \left. \left. - (vpi_2 + n \cdot vec^* e'_2) xGL_{2,j} + \frac{n^2}{2} (\sigma^\perp)^2 \right. \right. \\
&\quad \left. \left. \left. + b_{n-1}^{\$,num} \left(\tilde{B} \tilde{Z} + \begin{bmatrix} xGL_{1,i} \\ xGL_{2,j} \\ xGL_{3,k} \end{bmatrix}, \theta_0 \hat{s} + \theta_1 x + \theta_2 x^- + \lambda(\hat{s}) xGL_{1,i}, x \right) \right] \right] \right], \tag{A210}
\end{aligned}$$

We again use multi-linear interpolation and extrapolation to evaluate $b_{n-1}^{\$,num}$ and b_{n-1}^{num} at points that are not on the grid. We similarly implement the recursions (A166), (A168), and (A175) numerically to obtain risk-neutral bond and consumption claim valuations $B_n^{rn,num}$, $B_n^{rn,\$,num}$, $G^{rn,num}$.

D.2 Simulating the Model

We simulate a draw of length T . Results in Tables 2 and Table 4 use $T = 10000$ and discard the first 100 simulation periods to ensure that the system has reached the stochastic steady-state. We report model moments averaged across 2 independent simulations.

We use superscript *sim* to denote simulated quantities. We use the MATLAB function `mvrnd` to obtain independent draws $v_t^{sim} \sim N(0, \Sigma_v)$ for $t = 1, 2, \dots, T$. We then obtain the rotated shock according to $\epsilon_t^{sim} = A v_t^{sim}$ and $v_t^{LT,sim} = e_4 v_t^{sim}$. We generate draws for $\tilde{Z}_t^{sim}, t = 1, \dots, T$ by setting $\tilde{Z}_1^{sim} = 0$ and then updating according to (A96). We obtain the simulated non-rotated state vector for $t = 1, 2, \dots, T$ through the relation $Y_t^{sim} = A^{-1} \tilde{Z}_t^{sim}$. We generate draws for the surplus consumption ratio by setting $\hat{s}_1^{sim} = 0$ and $x_0^{sim} = 0$ and then updating according to (A105). We generate the simulated random walk component of inflation $v_t^*, t = 1, 2, \dots, T$ by starting from $v_1^{*sim} = 0$ and updating it according to equation (19) in the main paper. We initialize simulated log consumption

at $c_1^{sim} = 0$ and update it using (21). We then drop the first 100 simulation periods to allow the system to converge to the stochastic steady-state.

Having generated draws for the five state variables \tilde{Z}_t^{sim} , \hat{s}_t^{sim} , and x_{t-1}^{sim} , we obtain the simulated consumption-claim price-dividend ratio as $(P^c/C)_t^{sim} = F^{num}(\tilde{Z}_t^{sim}, \hat{s}_t^{sim}, x_{t-1}^{sim})$, n -period real bond prices as

$$P_{n,t}^{sim} = B_n^{num}(\tilde{Z}_t^{sim}, \hat{s}_t^{sim}, x_{t-1}^{sim}), \text{ and}$$

$B_{n,t}^{\$,sim} = B_n^{\$,num}(\tilde{Z}_t^{sim}, \hat{s}_t^{sim}, x_{t-1}^{sim})$. We obtain the corresponding risk-neutral valuation ratios by plugging into the risk-neutral asset pricing solutions:

$$(P^c/C)_t^{rn,sim} = F^{rn,num}(\tilde{Z}_t^{sim}, \hat{s}_t^{sim}, x_{t-1}^{sim}),$$

$$P_{n,t}^{rn,sim} = B_n^{rn,num}(\tilde{Z}_t^{sim}, \hat{s}_t^{sim}, x_{t-1}^{sim}), \text{ and}$$

$B_{n,t}^{rn,\$,sim} = B_n^{rn,\$,num}(\tilde{Z}_t^{sim}, \hat{s}_t^{sim}, x_{t-1}^{sim})$. We obtain nominal bond prices $P_{n,t}^{\$,sim}$ by combining $B_{n,t}^{\$,sim}$ and v_t^{*sim} according to (A127). We similarly obtain risk-neutral nominal bond prices $P_{n,t}^{rn,\$,sim}$ by combining $B_{n,t}^{rn,\$,sim}$ and v_t^{*sim} according to (A127).

To deal with the fact that \tilde{Z}_t^{sim} , \hat{s}_t^{sim} , x_{t-1}^{sim} are not usually on grid points we adopt a similar linear interpolation strategy as in the numerical evaluation of the asset pricing recursions described in Section D.1.3. We interpolate F^{num} , B_n^{num} , and $B_n^{\$,num}$ log-linearly. We simplify the interpolation strategy slightly compared to Section D.1.3. We use the MATLAB function `griddedInterpolant`, sacrificing some computational speed for simpler code. Even though rare events (and especially extremely negative realizations for \hat{s}) matter for the value function iteration in Section D.1.3, low-probability events have very little impact on the properties of simulated asset prices taking as given F^{num} , B_n^{num} , and $B_n^{\$,num}$. We therefore simplify the log-linear interpolation by truncating \tilde{Z}_t^{sim} , \hat{s}_t^{sim} , and x_{t-1}^{sim} at the maximum and minimum values covered by the grid.

Having generated $(\frac{P^c}{C})_t^{sim}$, $t = 1, \dots, T$, we compute log returns on the consumption claim $r_{t+1}^{c,sim}$ according to (A143). We obtain simulated price-dividend ratios for levered stocks by plugging into (A150). Finally, we obtain log bond yields and stock and bond excess returns as described in Section C.5.3. Risk-neutral bond and stock returns are computed by substituting $(\frac{P^c}{C})_t^{rn,sim}$, $P_{n,t}^{rn,\$,sim}$, and $P_{n,t}^{rn,sim}$ into the same relations.

We simulate pre-FOMC asset prices as follows. We use the MATLAB function `mvnrnd` to generate independent draws for the FOMC shock

$$v_t^{FOMC,sim} \sim N\left(0, \text{diag}\left(\left[0, 0, (\sigma_{ST}^{FOMC})^2, (\sigma_{LT}^{FOMC})^2\right]\right)\right), \text{ where } t = 1, \dots, T. \text{ Having}$$

drawn the FOMC shock $v_t^{FOMC,sim}$ we obtain the simulated pre-FOMC component of the overall quarterly simulated shock as

$$v_t^{pre,sim} = v_t^{sim} - v_t^{FOMC,sim}, \tag{A211}$$

$$\epsilon_t^{pre,sim} = A v_t^{pre,sim}. \tag{A212}$$

We then use the simulated values for \tilde{Z}_{t-1}^{sim} , Y_{t-1}^{sim} , c_{t-1}^{sim} , \hat{s}_{t-1}^{sim} , v_{t-1}^* and $\epsilon_t^{pre,sim}$ to compute the simulated pre-FOMC state vector according to equations (A180) through (A184). We then obtain pre-FOMC asset prices by substituting the simulated pre-FOMC state vector into equations (A185) through (A184). Simulated yield changes around FOMC news are then computed according to equations (A191) and (A194) and simulated FOMC stock returns are obtained according to equation (A196).

D.3 Parameter units

This subsection details the relation between parameter values in empirical (reported in the paper) and natural units (used for solving the code). We solve the model in natural units. However, it is most natural to report empirical moments and summary statistics in empirical units for interpretability.

For comparability with empirical moments, Table 1 reports model parameters in units that correspond to the output gap in annualized percent, and inflation and interest rates in annualized percent. As in [Campbell, Pflueger, and Viceira \(2020\)](#), we report the discount rate and the persistence of surplus consumption in annualized units. Concretely, Table 1 reports the following scaled parameters:

$$400 \times g, \tag{A213}$$

$$400 \times \bar{r}, \tag{A214}$$

$$\theta_0^4, \tag{A215}$$

$$\beta^4, \tag{A216}$$

$$4 \times \gamma^x \tag{A217}$$

$$100 \times \sigma_x, \tag{A218}$$

$$400 \times \sigma_\pi, \tag{A219}$$

$$400 \times \sigma_{ST}, \tag{A220}$$

$$400 \times \sigma_{LT}, \tag{A221}$$

$$\frac{1}{4} \times \psi, \tag{A222}$$

$$4 \times \kappa \tag{A223}$$

All other parameters reported in Table 1 do not need to be scaled.

E Details: Simulated Method of Moments

E.1 Reduced-Form Impulse Responses

This section describes how we estimate the macroeconomic impulse responses reported in Figure 2. We follow the procedure described below for both actual and simulated data, with the simulated data length matching the length of the empirical sample. Model impulse responses in Figures 2 are averaged over 100 simulations. In this section, we use subscripts IRF if variable names would otherwise be similar to different variables elsewhere in the paper.

To account for the unit root in inflation in the model, we estimate a vector error correction model of the form

$$Y_{IRF,t} = \Pi Y_{IRF,t-1} + \varepsilon_t \tag{A224}$$

where we define the vector for the VECM as:

$$Y_{IRF,t} = [x_{t-1}, \pi_t - \pi_{t-1}, i_t - \pi_t]. \quad (\text{A225})$$

This definition of the VAR(1) vector guarantees that each of the variables is stationary when the data is simulated from our model since the unit root affects the short-term interest rate i_t only through its effect on inflation π_t .

The shocks ε_t are not orthogonal and we denote their estimated variance-covariance matrix by Σ_ε . Next, we rotate the innovations to be orthogonal. This means that we need to re-write (A224) in the form:

$$R^{-1}Y_{IRF,t} = \Pi_R Y_{IRF,t-1} + \eta_t \quad (\text{A226})$$

where η_t is a vector of uncorrelated shocks, R is an invertible matrix, and $\Pi_R = R^{-1}\Pi$. We write the variance-covariance matrix of η_t as:

$$\Sigma_\eta = \mathbb{E}\eta_t'\eta_t = \begin{bmatrix} \sigma(\eta_1)^2 & 0 & 0 \\ 0 & \sigma(\eta_2)^2 & 0 \\ 0 & 0 & \sigma(\eta_3)^2 \end{bmatrix} \quad (\text{A227})$$

We pick R^{-1} to be lower-diagonal with ones along the diagonal. Having estimated Π and Σ_ε we obtain R , Π_R , and Σ_η using Cholesky factorization.

We then construct impulse responses. We start with a unit standard deviation orthogonalized shock to output gap:

$$\eta_1 = [\sigma(\eta_1), 0, 0] \quad (\text{A228})$$

which is equivalent to

$$\varepsilon_1 = R[\sigma(\eta_1), 0, 0]. \quad (\text{A229})$$

The n -th response to a one standard deviation shock to the output gap then is computed as:

$$\Pi^{n-1}\varepsilon_1 = \Pi^{n-1}R[\sigma(\eta_1), 0, 0]. \quad (\text{A230})$$

We can similarly compute the responses for the change in inflation $\pi_t - \pi_{t-1}$ and the difference between the nominal interest rate and inflation $i_t - \pi_t$. In order to then obtain the corresponding responses of inflation, we cumulate the responses of $\pi_t - \pi_{t-1}$ and finally add the response of inflation to that of $i_t - \pi_t$ to obtain the response of the short-term nominal interest rate.

E.2 Confidence intervals and objective function

We use a bootstrap method to compute confidence intervals for the empirical impulse responses shown in Figure 2 and for the variances of the impulse responses used in the SMM estimation. Let Π and Σ_ε denote the coefficient matrix and the variance-covariance matrix of shocks from estimating (A224) on actual data. We then generate bootstrapped data by simulating $Y_{IRF,t}^{boot}$ of identical sample length as the true data according to

$$Y_{IRF,t}^{boot} = \Pi Y_{IRF,t-1}^{boot} + \varepsilon_t^{boot}, \quad (\text{A231})$$

where ε_t^{boot} are drawn as iid normal with mean zero and variance-covariance Σ_ε . On the bootstrapped data, we then apply the methodology for IRFs described in Section E.1. That is, we re-estimate (A224) on the bootstrapped data and use the resulting estimates to construct bootstrapped impulse response functions. We generate 1000 independent bootstrap samples. Figure 2 shows confidence intervals, such that 95% of the time the bootstrapped impulse responses are within the interval.

For our objective function, we define the empirical target moments as follows. $\hat{\Psi}$ is $[15 \times 1]$. It includes $15 = 6 \cdot 3 - 3$ impulse responses. We have 15 impulse response moments, because we have nine impulse responses at zero (shock period), one, two, four, eight, and twelve quarters each. However, three of the shock period impulse responses are zero by our choice of orthogonalization and we exclude them from the objective function.

Let \hat{V} denote the bootstrapped variance-covariance matrix of $\hat{\Psi}^{boot} - \hat{\Psi}$. We then define the weighting matrix \hat{W} for the SMM objective function as the diagonal matrix with the inverse variances for the 15 impulse response moments along the diagonal:

$$\hat{W} = \text{diag}(\text{inv}(\hat{V}_{1,1}), \text{inv}(\hat{V}_{2,2}), \dots, \text{inv}(\hat{V}_{51,51})). \quad (\text{A232})$$

The SMM objective function is then given by equation (40) in the main text.

E.3 Grid search

We minimize the objective function $J(\sigma)$ using a two-step grid search. To reduce the need to compute (computationally expensive) asset prices along the grid, we separate the parameters into $[\sigma_x, \sigma_\pi, \sigma_{ST}]$ and σ_{LT} . The first step of the grid search finds the parameter values for $[\sigma_x, \sigma_\pi, \sigma_{ST}]$ that minimize the objective function while holding the volatility of the long-term monetary policy shock constant at $\sigma_{LT} = 0.25$, which we have chosen to match roughly the volatility of changes in 10-on-10-year breakeven, which equals 0.26% in our empirical sample. In this first grid search step, we solve and simulate macroeconomic dynamics and reduced-form impulse responses (but not asset prices) over a grid for the first three volatility parameters. We choose an equally-spaced grid with 20 points between 0.01 and 1 for each of σ_x , σ_π , and σ_{ST} , so we evaluate the macroeconomic dynamics at a total of $20^3 = 8000$ gridpoints in this step. We discard parameter values in this step, where asset prices do not exist.

In a second step, we find the volatility of the long-term monetary policy shock σ_{LT} by minimizing the distance between the volatility of changes in 10-on-10 year breakeven in the model and in the data, while holding all other model parameters constant. This second step requires solving for asset prices at each grid point, and is hence substantially slower than the first step. We evaluate the model volatility of changes in 10-on-10-year breakeven inflation on an equally-spaced grid for σ_{LT} with 20 points between 0.01 and 1. Because it takes about 2 minutes to solve for macroeconomic dynamics and asset prices, this second step of the grid search takes about $2 \times 20 = 40$ minutes. We again discard parameter vectors where asset prices do not exist.

F Additional Model Results

F.1 Switching off model components

Table A1 shows that the model results described in Table 4 are robust to switching off individual types of shocks. For instance, reducing the equilibrium volatility of Phillips curve, short-term monetary policy, or long-term monetary policy shocks leaves the relationship of stock returns and monetary policy surprises on FOMC dates unchanged. For the counterfactual exercises in columns (5) and (6) of Table A1 monetary policy shocks on FOMC dates are still non-zero, but they are unanticipated and out-of-equilibrium because the equilibrium volatility of monetary policy shocks set to zero.

Setting the quarterly equilibrium volatility of markup shocks, short-term monetary policy shocks, or long-term monetary policy shocks to zero has no qualitative or even quantitative impact on the coefficients of interest in panels A and B. Switching off the habit shock in column (2) even increases the model slope coefficients around FOMC announcements, and the risk premium response. Intuitively, in the absence of independent habit shocks the consumption claim is conditionally perfectly correlated with surplus consumption, so stocks are even riskier for investors.

Table A2 does a similar robustness exercise for the calibrated parameter values. It shows that the stock return response to monetary policy surprises and, in particular, the share of this response attributed to time-varying risk premia, is robust to varying the calibrated parameters within ranges that are within reasonable priors. Column (2) shows that increasing the capital share from $\tau = 0.33$ to $\tau = 0.5$ does not change our central result in Table 4. Column (3) shows that assuming lower price stickiness of $\alpha = 0.5$ (and hence a lower average of prices) rather than $\alpha = 0.67$ (as in our baseline) does not change our central results. Column (4) shows that assuming $\theta = 8$ (corresponding to lower steady-state markups of 15%) rather than $\theta = 6$ (as in our baseline) leaves results unchanged. Column (5) shows that lowering the Frisch elasticity of labor supply to 0.5 (relative to 1.0 in our baseline) leaves our results unchanged. Columns (6) and (7) show that changing the weight the monetary policy rule puts on the output gap (raising γ_x to 1.0 compared to 0.5 in our baseline) or the weight that it puts on inflation (lowering γ_π to 1.1 from 1.5 in our baseline) makes no difference. Column (8) changes the role of monetary policy persistence and shows that results are unchanged if monetary policy is perceived to put lower weight on lagged interest rates and we switch of the link between interest rate and future expected productivity growth.

Table A1: Switching off Individual Shocks

	(1)	(2)	(3)	(4)	(5)
	Baseline	$\sigma_x = 0$	$\sigma_\pi = 0$	$\sigma_{ST} = 0$	$\sigma_{LT} = 0$
Panel A: Overall monetary policy shocks effect					
Slope(S&P 500 Return, Fed Funds)	-5.27	-15.43	-5.15	-4.96	-5.20
Slope(S&P 500 Return, 10Y Breakeven)	5.89	17.00	5.74	5.54	5.81
Panel B: Monetary policy shocks effect on risk premia					
Slope(S&P 500 Risk Premium, Fed Funds)	-2.54	-14.16	-2.49	-2.21	-2.46
Slope(S&P 500 Risk Premium, 10Y Breakeven)	2.7	15.34	2.64	2.35	2.63
Panel C: Bond Betas					
Real Bond-Stock Beta	0.03	0.17	0.02	-0.02	0.01
Breakeven-Stock Beta	-0.13	-0.22	-0.13	-0.11	-0.04

Note: This table compares asset pricing moments while switching off shocks one at a time. The real and breakeven stock betas are computed as in Table 2, and the asset price reactions around monetary policy dates are as in Table 4. Column (1) of Panel A repeats the model regression of Table 4, column (2). The remaining columns of Panel A report the corresponding model regression coefficients while switching off individual model components. Panel B reports regression estimates corresponding to Table 4, column (4), where the dependent variable is the risk premium component of equity returns. For all panels, column (1) repeats the baseline model results. Column (2) sets the habit shock volatility to zero. Column (3) sets the markup shock volatility to zero. Column (4) sets the short-term monetary policy shock volatility to zero. Column (6) sets the long-term monetary policy shock volatility to zero. For the counterfactual exercises in columns (4) and (5) of Table A1 monetary policy shocks on FOMC dates are still non-zero, but they are unanticipated and out-of-equilibrium because the equilibrium volatility of monetary policy shocks set to zero. All other parameters are held constant at the values listed in Table 1.

Table A2: Robustness to Parameter Values

	(1)	(2)	(3)	(4)	(5)	(6)	(7)	(8)
	Baseline	$\tau = 0.5$	$\alpha = 0.5$	$\theta = 8$	Frisch= 0.5	$\gamma_x = 1$	$\gamma_\pi = 1.1$	$\rho^i = 0.8, \rho_a = 0$
Panel A: Overall monetary policy shocks effect								
Slope(S&P 500 Return, Fed Funds)	-5.27	-5.12	-4.81	-5.20	-5.11	-4.59	-6.09	-6.34
Slope(S&P 500 Return, 10Y Breakeven)	5.89	5.73	5.10	5.95	5.73	4.95	6.28	6.88
Panel B: Monetary policy shocks effect on risk premia								
Slope(S&P 500 Risk Premium, Fed Funds)	-2.54	-2.42	-2.21	-2.47	-2.42	-2.03	-2.93	4.14
Slope(S&P 500 Risk Premium, 10Y Breakeven)	2.7	2.56	2.29	2.63	2.56	2.06	2.89	4.27
Panel C: Bond Betas								
Real Bond-Stock Beta	0.03	0.03	0.02	0.03	0.03	0.00	0.05	-0.02
Breakeven-Stock Beta	-0.13	-0.13	-0.17	-0.12	-0.13	-0.13	-0.15	-0.10

Note: This table compares asset pricing moments while varying individual parameter values. The real and breakeven stock betas are computed as in Table 2, and the asset price reactions around monetary policy dates are as in Table 4. Column (1) of Panel A repeats the model regression of Table 4, column (2). The remaining columns of Panel A report the corresponding model regression coefficients while setting individual parameters to the values noted in the top row. All other parameters are held constant at the values listed in Table 1.

F.2 Model Real Bond Yields around FOMC Announcements

In this Appendix Section, we show that our model matches the comovement between the short-term nominal interest rate and long-term real bond yields around FOMC dates. Note that this result is different from the empirical evidence in [Hanson and Stein \(2015\)](#) and [Nakamura and Steinsson \(2018\)](#), who use different measures of monetary policy shocks based on somewhat more long-term nominal interest rates. By contrast, we match the long-term real bond yield response to very traditional monetary policy shocks based on surprises to the (very short term) Federal Funds rate.

Table A3: Data and Model Real Bond Yields around FOMC Announcements

	(1) Data	(2) Model	(3) Model ($\rho^a = 0$)
Slope(5Y Real Yield, Fed Funds)	0.42* (0.22)	0.36	0.32
Risk Neutral		0.35	0.29
Slope(10Y Real Yield, Fed Funds)	0.28* (0.16)	0.17	0.18
Risk Neutral		0.17	0.15

Note: This table compares the comovement of long-term real bond yields and short-term nominal interest rates around monetary policy announcements in the model and in the data. The table reports coefficient estimates from regressions of the form $\Delta^{FOMC}y_{n,t} = b_0 + b_1\Delta^{FOMC}i_t + \varepsilon_t$, where $\Delta^{FOMC}y_{n,t}$ is either the change in the 10-year or 5-year real bond yield from the day before the FOMC announcement to the day after. We use zero-coupon TIPS yields from [Gürkaynak, Sack, and Wright \(2010\)](#). The surprise in the Federal Funds rate and the sample are as in [Table 4](#). Model asset price changes around FOMC announcements are also as described in [Table 4](#). Risk neutral rows show the slope coefficients when model long-term real bond yields are computed from the stochastic discount factor of a risk neutral investor taking macroeconomic dynamics as given.

[Table A3](#) shows that our model matches the empirical relationship between long-term real yields and short-term nominal yields on FOMC days:

$$\Delta^{FOMC}y_{n,t} = b_0 + b_1\Delta^{FOMC}i_t + \varepsilon_t, \quad (\text{A233})$$

where $\Delta^{FOMC}y_{n,t}$ is the change in either the 10-year or the 5-year real bond yield and $\Delta^{FOMC}i_t$ is the change in the Federal Funds rate. [Table A3](#), column (1) shows that long-term real bond (TIPS) yields indeed move with surprises in short-term interest rates in our sample, consistent with prior empirical results. In the data, a 25 bps surprise increase in the short-term nominal interest rate tends to be accompanied by a substantial 11 bps increase in the 5-year TIPS yield and a 7 bps increase in the 10-year TIPS yield.

Column (2) shows that the model replicates the positive empirical relationship between long-term real bond yields and short-term nominal yields on FOMC dates. In the model, a 25 bps point increase in short-term nominal yield is associated with a 9 bps increase in the 5-year real bond yield, and a 4 bps increase in the 10-year real bond yield,

similarly to the data. Both of these coefficients are economically meaningful and within two standard deviations of the empirical estimates, though smaller than in the data.

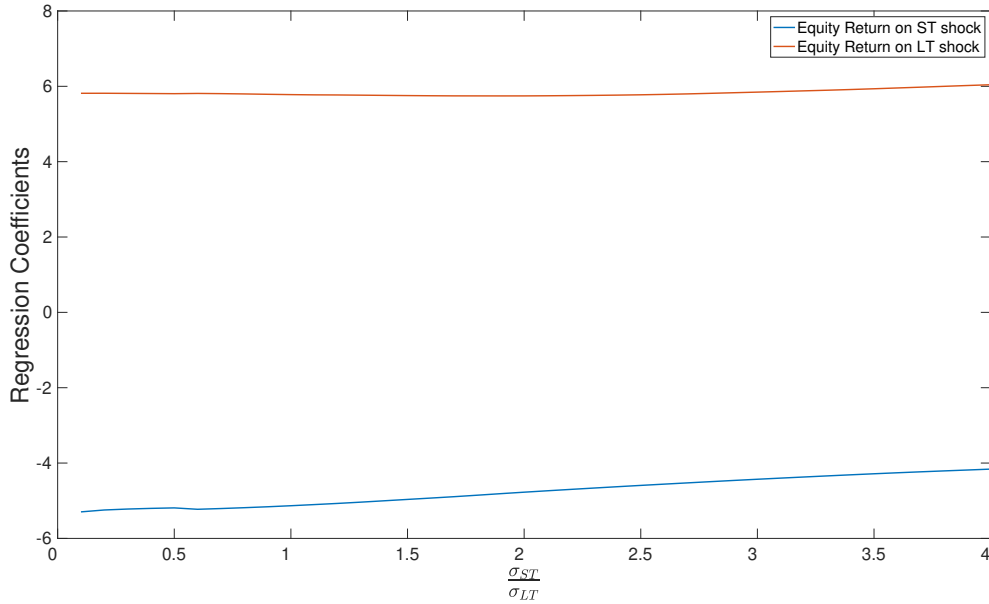
F.3 Robustness Model FOMC Results

Table 4 and Figure 5 report the slope coefficients b_1 and b_2 from running the following regression on simulated model data

$$r_t^{\delta, FOMC} = b_0 + b_1 \Delta i_t^{FOMC} + b_2 \Delta breakeven_{n,t} + \varepsilon_t. \quad (A234)$$

For our main results, we pick standard deviations for the ST and LT monetary policy shocks on FOMC days to match the empirical standard deviations of our respective proxies for those shocks: 4.3 bps and 3.3 bps. To make sure that our model results on the relationship of monetary policy shocks and equity returns are not driven by the relative volatilities of short-term and long-term monetary policy shocks, in Figure A1 we plot the estimates for b_1 and b_2 while varying $\sigma_{ST}^{FOMC} / \sigma_{LT}^{FOMC}$.

Figure A1: Model High-Frequency Regression Coefficients against Volatility of FOMC ST Monetary Policy Shock

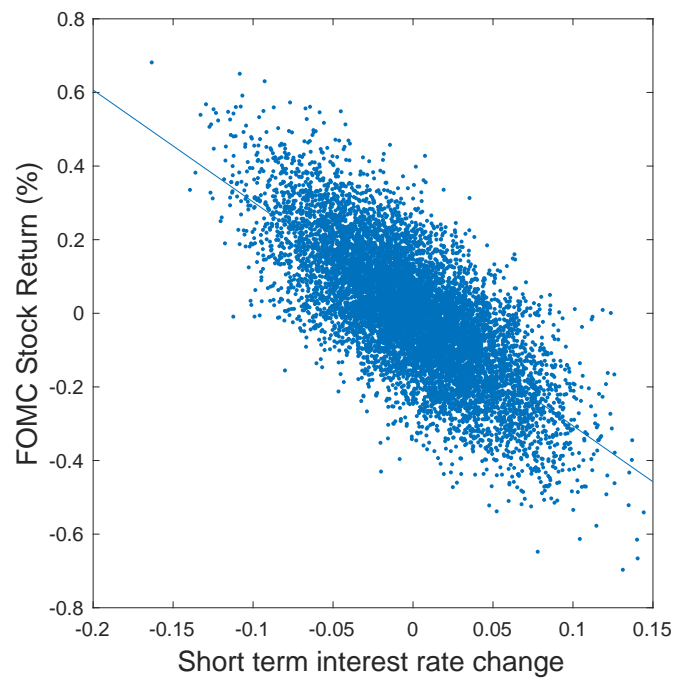


Note: This figure shows regression coefficients b_1 and b_2 from the model regression (A234), also shown in column (2) in Table 4 in the main paper. Each dot in the figure corresponds to a model simulation with a different value for the volatility of short-term monetary policy shocks realized on FOMC dates σ_{ST}^{FOMC} . We hold the volatility of the long-term monetary policy shock realized on FOMC dates constant at its baseline value of $\sigma_{LC}^{FOMC} = 3.3$ bps. We plot the model regression coefficients b_1 and b_2 on the y-axis against the ratio of the short-term to long-term monetary policy shocks realized on FOMC dates $\frac{\sigma_{ST}^{FOMC}}{\sigma_{LT}^{FOMC}}$ on the x-axis.

F.4 Shape of Bernanke-Kuttner relationship

In this section we show that the model relationship between equity returns and short-term interest rate surprises on FOMC days, documented in Table 4, displays no obvious asymmetries for positive vs. negative monetary policy surprises. This can be seen from a scatter plot of model stock returns and short-term interest rate surprises in Figure A2. This figure shows simulated short-term interest rate changes and stock returns on FOMC dates in the model. While the model implies a nonlinear relationship between log surplus consumption and stock prices over the full state space, the relationship between state variables and stock prices is nonetheless smooth, leading to a locally linear relationship near the steady-state. This leads to a symmetric relationship between empirically plausible surprises to the short-term interest rate and stock returns, whereby negative monetary policy surprises have approximately similar magnitude effects as positive monetary policy surprises.

Figure A2: Scatter Plot of FOMC Stock Returns and Short-Term Interest Rate Surprise in Model



G Additional Empirical Results

G.1 Breakeven Liquidity and the Treasury-TIPS Basis

In this section we show that the positive correlation between equity returns and changes in the 10 year breakeven rate are not driven by changes in the Treasury-TIPS Basis (Gürkaynak, Sack, and Wright, 2010; Fleckenstein, Longstaff, and Lustig, 2014).

Firstly, in Figure A3 below we show that the relationship is essentially the same if we use daily changes in the 10 year inflation swap rate instead (USSWIT10 from Bloomberg) of the breakeven.

Even more directly, we can check if the Treasury-TIPS basis moves systematically with equity returns on FOMC days. To do this, we construct a simple proxy for the Treasury-TIPS basis by subtracting the 10-year inflation swap rate from the corresponding breakeven rate. We then regress the equity returns on FOMC days on changes in the Treasury-TIPS basis and report the result in Table A4. As the result shows, there is no significant correlation between the two changes, on FOMC dates. Therefore, the relationship between inflation breakevens and equity returns on FOMC days, which we document in the right panel of Figure 1, is not driven by changes in the Treasury-TIPS basis.

Table A4: FOMC equity returns and the Treasury-TIPS Basis

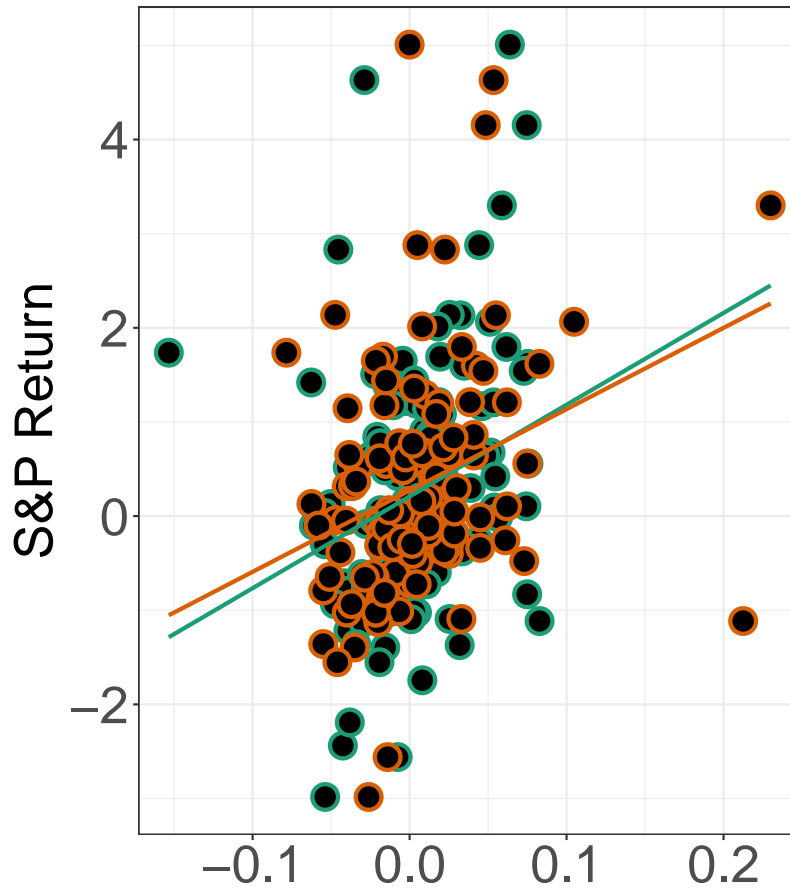
	SPY Return
Treasury-Tips Basis Change	-3.84 (6.09)
Observations	122
Adjusted R ²	0.00

Note: This table shows the slope estimate from a regression of the form:

$$r_t^{FOMC} = b_0 + b_1(\Delta^{FOMC}b_{10,t} - \Delta^{FOMC}infSwap_{10,t}) + \varepsilon_t.$$

$\Delta^{FOMC}infSwap_{10,t}$ is the daily change in the inflation swap rate and $\Delta^{FOMC}b_{10,t}$ is the daily change in the 10-year breakeven rate, defined as the difference between 10-year nominal and 10-year real bond yields. The breakeven rate is the difference between the 10-year nominal Treasury yield and 10-year TIPS yield from Gürkaynak, Sack, and Wright (2007, 2010). The inflation swap data is from Bloomberg. The green and orange lines are linear regression best fit lines. The sample of scheduled FOMC days is from the start of 2001 until March 2019. The data begins from the start of 2003 since this is when the TIPS data start. Heteroskedasticity adjusted standard errors are reported in parentheses below the estimates. *p<0.1; **p<0.05; ***p<0.01

Figure A3: FOMC Equity Returns against Breakeven and Inflation swaps changes



● 10Y Breakeven ● 10Y Inflation Swap

Note: This figure shows the relationship of the daily change in 10-year breakeven inflation rates (in green) and 10-year inflation swap changes (in orange) with daily S&P 500 returns where each data point corresponds to a FOMC meeting. The breakeven rate is the difference between the 10-year nominal Treasury yield and 10-year TIPS yield from [Gürkaynak, Sack, and Wright \(2007, 2010\)](#). The inflation swaps data is from Bloomberg. The green and orange lines are linear regression best fit lines. The sample of scheduled FOMC days is from the start of 2001 until March 2019. The data begins from the start of 2003 since this is when the TIPS data start.

G.2 High-frequency breakeven changes on FOMC dates

We next repeat the empirical analysis in Table 3 using intraday data for inflation swaps to address concerns about noise from using 1-day changes in breakeven. For the main analysis, we are not able to use higher frequency intraday data as intraday data for inflation swaps only becomes available in 2012. We obtain intraday data for 10-year inflation swaps from Bloomberg starting in 2012. We compute the 1-hour change in the 10-year inflation swap to match the time interval for the Federal Funds rate shock and intraday stock returns. In Table A5 below, we regress intraday stock returns on the intraday Federal Funds rate shock and these intraday changes in 10-year inflation swap rates. We find that the estimates are consistent with those reported in Table 3 both in sign and in magnitude, though the statistical significance is reduced.

Table A5: Empirical High-Frequency Stock Returns on FOMC Dates

	<i>Dependent variable:</i>			
	S&P 500 Return			10Y Breakeven
	(1)	(2)	(3)	(4)
FF Shock	-14.03 (8.92)		-13.12 (8.09)	-0.14 (0.09)
10Y Breakeven		11.29 (19.07)	6.68 (16.22)	
Constant	0.02 (0.09)	0.06 (0.08)	0.03 (0.08)	-0.001 (0.001)
Observations	58	58	58	58
R ²	0.09	0.02	0.09	0.05
Adjusted R ²	0.07	0.004	0.06	0.03

Note: Columns (1) to (3) show regressions of the form: $r_t^{FOMC} = b_0 + b_1 \Delta^{FOMC} i_t + b_2 \Delta^{FOMC} b_{10,t} + \varepsilon_t$. $\Delta^{FOMC} i_{n,t}$ is the change in the Federal Funds rate in the one hour around FOMC announcements and $\Delta^{FOMC} b_{10,t}$ is the change in the 10-year inflation swap rate in the same hourly window. We include these variables separately in columns (1) and (2), and jointly in column (3). The data on Federal Fund rate surprises is from [Gorodnichenko and Weber \(2016\)](#), inflation swap data is obtained from Bloomberg (ticker USSWIT10), and one hour S&P 500 returns are from TAQ data. Column (4) reports a regression of the form $\Delta^{FOMC} b_{10,t} = b_0 + b_1 \Delta^{FOMC} b_{n,t} + \varepsilon_t$. Our sample consists of scheduled FOMC days from January 2012 up to March 2019. Heteroskedasticity adjusted standard errors are reported in parentheses below the estimates. *p<0.1; **p<0.05; ***p<0.01

G.3 Effect of monetary policy during the post-crisis period

Our model predicts that stock returns should be more sensitive to monetary policy news following a sequence of bad shocks when the price-dividend ratio is low, such as during a crisis. In this section we tabulate the properties of stock returns in narrow windows around FOMC announcements during the post-crisis period (defined as October 2008 through March 2019).

Table A6 regresses stock returns onto Federal Funds rate surprises and breakeven changes around FOMC announcements for this subsample. The regression is analogous to Table 3, except that we would expect to find larger coefficients given that this period was characterized by a deep recession with a slow recovery and the lowest price-dividend ratios in our sample. This prediction is confirmed in the data. Stock returns respond to surprises in the Federal Funds rate and 10-year breakeven 50% more strongly than for the full sample. In terms of magnitude, this post-crisis period yields a coefficient onto Federal Funds rate surprises of around negative 7.5 and a coefficient onto breakeven surprises of around positive 7.5, in line with the regression coefficients predicted by the model when the surplus consumption ratio is within the bottom 30% of its distribution.

Table A6: Post-Crisis Stock Returns on FOMC Dates

	<i>Dependent variable:</i>		
	S&P 500 Return		
	(1)	(2)	(3)
FF Shock	-10.90** (3.39)		-7.59** (3.39)
10Y Breakeven		8.64** (2.36)	7.55** (2.26)
Constant	0.05 (0.08)	0.01 (0.07)	0.00 (0.07)
Observations	84	84	84
R ²	0.09	0.17	0.21

Note: Regressions are analogous to Table 3 columns (1) through (3), except that this table uses the post-crisis subsample (October 2008 through March 2019). Robust standard errors in parentheses. Significance at the 1% and 5% levels are indicated by * and **.

APPENDIX REFERENCES

- Campbell, John Y, and John H Cochrane, 1999, By force of habit, *Journal of Political Economy* 107, 205-251.
- Campbell, John Y, Carolin Pflueger, and Luis M Viceira, 2020, Macroeconomic drivers of bond and equity risks, *Journal of Political Economy* 128, 3148–3185.
- Cogley, Timothy, and Argia M. Sbordone, 2008, The time-varying volatility of macroeconomic fluctuations, *American Economic Review* 98, 2101–2126.
- Greenwood, Jeremy, Zvi Hercowitz, and Gregory W Huffman, 1988, Investment, capacity utilization, and the real business cycle, *American Economic Review* pp. 402–417.
- Hanson, Samuel G, and Jeremy C Stein, 2015, Monetary policy and long-term real rates, *Journal of Financial Economics* 115, 429–448.
- Nakamura, Emi, and Jón Steinsson, 2018, High-frequency identification of monetary nonneutrality: the information effect, *Quarterly Journal of Economics* 133, 1283–1330.
- Smets, Frank, and Rafael Wouters, 2007, Shocks and frictions in us business cycles: A Bayesian DSGE approach, *American Economic Review* pp. 586–606.
- Wachter, Jessica A., 2005, Solving models with external habit, *Finance Research Letters* 2, 210–226.
- Walsh, Carl E, 2017, *Monetary theory and policy* (MIT press).
- Woodford, Michael, 2003, *Interest and Prices* (Princeton University Press)